Title

Identification of Novel Kaposi's Sarcoma-Associated Herpesvirus Orf50 Transcripts: Discovery of New RTA Isoforms with Variable Transactivation Potential

Journal

Journal of Virology, 91(1)

ISSN

0022-538X

Authors

Wakeman, Brian S
Izumiya, Yoshihiro
Speck, Samuel H

Publication Date

2017

DOI

10.1128/jvi.01434-16

Peer reviewed

AMERICAN SOCIETY FOR MICROBIOLOGY | Journal of Virology®

Identification of Novel Kaposi's Sarcoma-Associated Herpesvirus *Orf50* Transcripts: Discovery of New RTA Isoforms with Variable Transactivation Potential

Brian S. Wakeman,[a] Yoshihiro Izumiya,[b] Samuel H. Speck[a]

Emory Vaccine Center and Department of Microbiology and Immunology, Emory University School of Medicine, Atlanta, Georgia, USA[a]; Department of Dermatology, University of California Davis School of Medicine, Sacramento, California, USA[b]

ABSTRACT Kaposi's sarcoma-associated herpesvirus (KSHV) is a gammaherpesvirus that has been associated with primary effusion lymphoma and multicentric Castleman's disease, as well as its namesake Kaposi's sarcoma. As a gammaherpesvirus, KSHV is able to acutely replicate, enter latency, and reactivate from this latent state. A key protein involved in both acute replication and reactivation from latency is the replication and transcriptional activator (RTA) encoded by the gene *Orf50*. RTA is a known transactivator of multiple viral genes, allowing it to control the switch between latency and virus replication. We report here the identification of six alternatively spliced *Orf50* transcripts that are generated from four distinct promoters. These newly identified promoters are shown to be transcriptionally active in 293T (embryonic kidney), Vero (African-green monkey kidney epithelial), 3T12 (mouse fibroblast), and RAW 264.7 (mouse macrophage) cell lines. Notably, the newly identified *Orf50* transcripts are predicted to encode four different isoforms of the RTA which differ by 6 to 10 residues at the amino terminus of the protein. We show the global viral transactivation potential of all four RTA isoforms and demonstrate that all isoforms can transcriptionally activate an array of KSHV promoters to various levels. The pattern of transcriptional activation appears to support a transcriptional interference model within the Orf50 region, where silencing of previously expressed isoforms by transcription initiation from upstream Orf50 promoters has the potential to modulate the pattern of viral gene activation.

IMPORTANCE Gammaherpesviruses are associated with the development of lymphomas and lymphoproliferative diseases, as well as several other types of cancer. The human gammaherpesvirus, Kaposi's sarcoma-associated herpesvirus (KSHV), is tightly associated with the development of Kaposi's sarcoma and multicentric Castleman's disease, as well as a rare form of B cell lymphoma (primary effusion lymphoma) primarily observed in HIV-infected individuals. RTA is an essential viral gene product involved in the initiation of gammaherpesvirus replication and is conserved among all known gammaherpesviruses. We show here for KSHV that transcription of the gene encoding RTA is complex and leads to the expression of several isoforms of RTA with distinct functions. This observed complexity in KSHV RTA expression and function likely plays a critical role in the regulation of downstream viral and cellular gene expression, leading to the efficient production of mature virions.

KEYWORDS Kaposi's sarcoma-associated herpesvirus, RTA isoforms, alternative promoter usage, alternative splicing, transcriptional activation

Received 18 July 2016 **Accepted** 14 October 2016

Accepted manuscript posted online 19 October 2016

Citation Wakeman BS, Izumiya Y, Speck SH. 2017. Identification of novel Kaposi's sarcoma-associated herpesvirus *Orf50* transcripts: discovery of new RTA isoforms with variable transactivation potential. J Virol 91:e01434-16. https://doi.org/10.1128/JVI.01434-16.

Editor Jae U. Jung, University of Southern California

Address correspondence to Samuel H. Speck, sspeck@emory.edu.

Herpesviruses are large double-stranded DNA viruses that encode a variety of proteins required for acute replication and maintenance within a host during latency. Latency is the hallmark of herpesvirus infections and results in a lifelong persistence of virus infection that cannot be cleared. This lifelong infection is marked by sporadic viral reactivation, resulting in viral replication and reseeding of latency reservoirs. One important member of the herpesvirus family is the gammaherpesvirus Kaposi's sarcoma-associated herpesvirus (KSHV). This gammaherpesvirus is associated with the development of a variety of conditions, such as Kaposi's sarcoma, multicentric Castleman's disease, and primary effusion lymphoma (PEL). Although the seroprevalence of KSHV is not as dramatic as that of another human gammaherpesvirus, Epstein-Barr virus (EBV), still between 5 and 20% of individuals, depending on the geographical location, are latently infected with KSHV by adulthood (1–4). While KSHV-associated malignancies are rare, especially in immunocompetent individuals, people who are immunocompromised—either as a result of HIV infection or because of immunosuppressive drug therapies—run a higher risk of KSHV-associated complications (5–10).

The known gammaherpesviruses, in general, exhibit a narrow host tropism and are associated with lymphoproliferative diseases and lymphomas. Furthermore, gammaherpesviruses are well represented within the mammalian kingdom; examples have been found in humans and in nonhuman primates, rodents, sheep, horses, seals, dolphins, kangaroos, and cats (11–14). Notably, these viruses all share large degrees of genetic and functional homology (15, 16). One of the most highly conserved genes among gammaherpesviruses is the *Orf50* gene encoding RTA (replication and transcriptional activator), a viral protein essential for gammaherpesvirus replication and reactivation from latency (17–19). Lytic replication requires a cascade of gene expression, which leads to viral DNA replication and the assembly and release of newly formed infectious virions (20). The RTA protein is a strong transactivator of downstream viral genes, as evidenced by its ability when ectopically expressed in cells harboring a latent gammaherpesvirus genome(s) to initiate reactivation from latency and entry into the lytic gene expression cascade (21–24). The transactivation potential of RTA has been demonstrated for a variety of downstream targets in both KSHV and the rodent virus murine gammaherpesvirus 68 (MHV68). For example, KSHV RTA has been shown to transactivate Orf57, K12, PAN, K5, K1, and K8 genes, as well as to transactivate its own promoter (21, 25–31). A comprehensive screening of RTA activity has revealed that transcription of many viral genes is upregulated (32). In addition, RTA has been shown to target a number of cellular genes; for example, RTA has been shown to bind and upregulate the interleukin-6 (IL-6) promoter (33, 34).

With the impact that RTA expression has on the viral life cycle, it is likely that the expression of RTA is highly regulated by a variety of mechanisms. Recently, we have used MHV68 as a model of gammaherpesvirus replication and have determined that transcription of the Orf50 region is much more complex than previously appreciated. From studies in which we disrupted the known Orf50 promoter, it became apparent that there were alternative transcription initiation sites for Orf50 expression (35, 36). Ultimately, this revealed the presence of three additional upstream transcription initiation sites driving alternatively spliced Orf50 transcripts (36). Notably, all of these alternatively spliced transcripts splice to the previously identified E1 exon, which in turn is spliced to the E2 exon that encodes the bulk of the RTA protein. As previously described, open reading frame 50 (ORF50) is significantly extended upstream by the E1 to E2 exon splice by virtue of the presence of a short, in-frame ATG initiated reading frame at the 3′ end of the E1 exon (37, 38) (Fig. 1A). Notably, all of the alternatively spliced RTA transcripts encode a single RTA isoform (36). The importance of alternative RTA promoters recently became apparent from studies of helminth infection, where it was shown that IL-4 induction led to MHV68 reactivation and that the action of IL-4 mapped to one of the distal RTA promoters (39).

We demonstrate here that, like MHV68, the expression of RTA in the human gammaherpesvirus KSHV is also encoded from multiple alternatively spliced transcripts

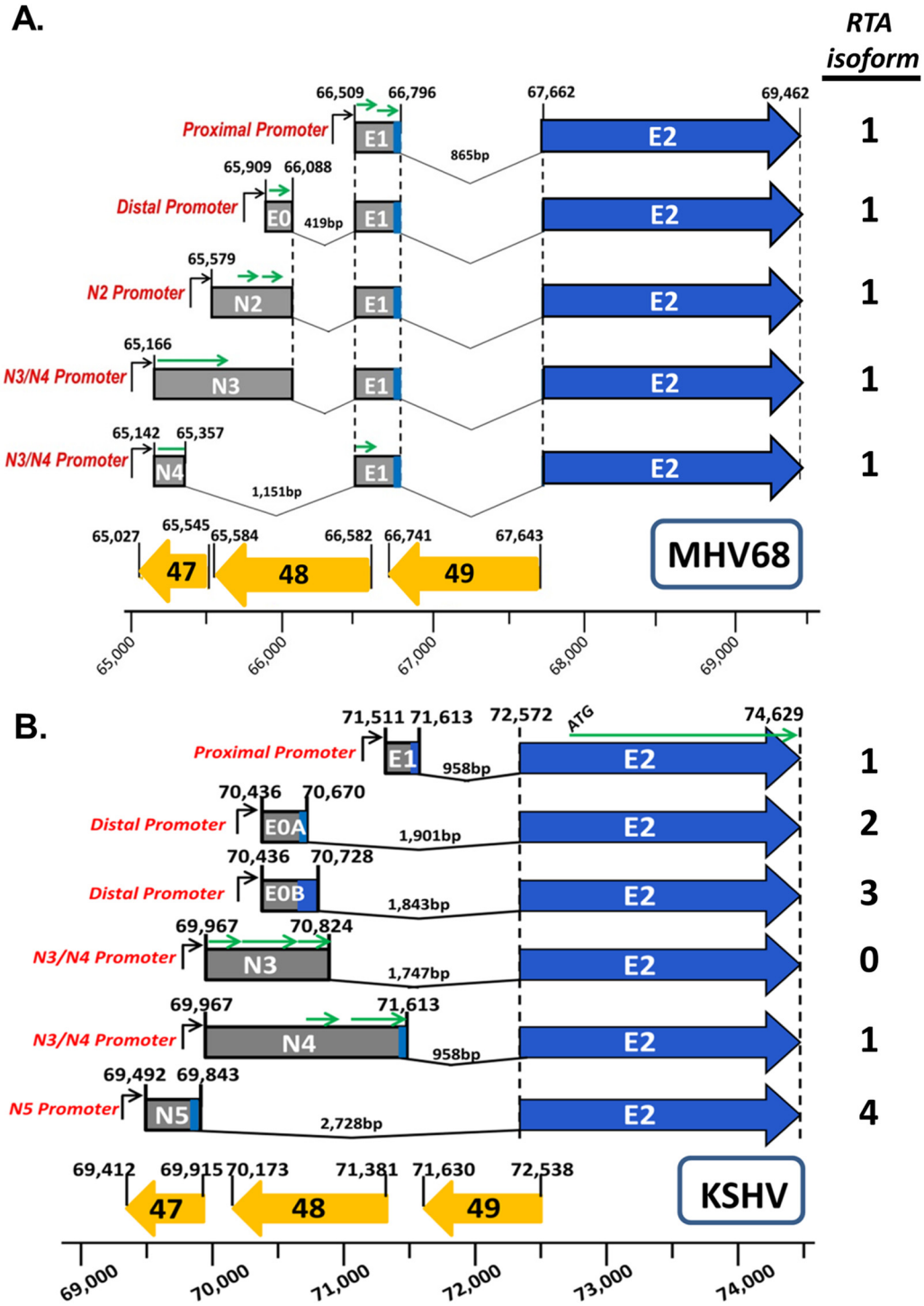

FIG 1 Genomic map demonstrating Orf50 transcripts, splicing, and reading frames of both MHV68 and KSHV. (A) Previously identified MHV68 genome (36) showing five unique Orf50 transcripts driven from four different promoters all encoding a single RTA protein isoform. (B) RACE analyses and primer walking of the KSHV Orf50 region performed using cDNAs generated from TPA-induced BCBL-1 KSHV PEL cell lines at 24 and 48 h postinfection. 5′ RACE analysis by nested PCR was performed using reverse primers located in E2 in conjunction with universal 5′ RACE forward primers. Primer walking was conducted using reverse primers located in E2 in conjunction with a series of forward primers at 50-bp intervals located upstream of previously identified transcripts. Experiments revealed the presence of six transcripts with five unique splicing events to the large E2 exon. Exon E1 is a 102-bp exon splicing out a 958-bp intron and extending the E2 ORF by 6 amino acids, while generating RTA isoform 1. Exon E0A is a 234-bp exon splicing out a 1,901-bp intron and extending the E2 ORF by 6 amino acids, while generating RTA isoform 2. Exon E0B is a 292-bp exon splicing out a 1,843-bp intron and extending the E2 ORF by 10 amino acids, while generating RTA isoform 3. Exon N3 is a noncoding 857-bp exon splicing out a 1,747-bp intron, while not extending the E2 ORF. Exon N4 is a 1,646-bp exon splicing out the same 958-bp intron as exon 1, resulting in the generation of RTA isoform 1. Finally, exon N5 is a 351-bp exon splicing out

(Continued on next page)

that are expressed from four distinct promoters. However, unlike MHV68, alternative splicing from the unique upstream exons to the major Rta coding exon (E2 exon) results in the generation of four different RTA isoforms that contain unique 6- to 10-amino-acid sequences at their amino termini. The transcriptional activation potential of these different Rta isoforms is presented, and the potential impact that these different Rta isoforms may have on KSHV replication is discussed.

RESULTS

Identification of additional KSHV *Orf50* transcripts. The Orf50 region is highly conserved among all gammaherpesvirus family members. We have previously shown that transcription of KSHV Orf50 is driven by two distinct promoters: the proximal promoter (also referred to as the Orf50 E1 promoter), encoding a short 102-bp exon, E1, which splices to the large 2,057-bp exon, E2; and the distal promoter (also referred to as the Orf50 E0 promoter), which drives expression of two distinct alternatively spliced transcripts, one that contains a short 234-bp exon (E0A) and a second one that contains a slightly longer 292-bp exon (E0B), both of which splice to the large 2,057-bp exon E2 (35). It was further shown that this organization of the Orf50 region, and the use of two distinct promoters, was also conserved in the other human gammaherpesvirus EBV and the rodent gammaherpesvirus MHV68 (35). As discussed above, we have extended the finding in MHV68, identifying the existence of additional promoters driving RTA expression (36). In addition to the proximal and distal promoters driving MHV68 Rta expression, there are also two other promoters driving the transcription of three unique transcripts: the N3 promoter driving the transcription of the N3 transcript, and the N4/N5 promoter, which drives expression of two different alternatively spliced transcripts: the N4 transcript and the N5 transcript (see the schematic illustration in Fig. 1A). Notably, to date, all of the identified *Orf50* transcripts encoded by MHV68 contain the E1 exon, which splices directly to the E2 exon and thus encodes a single Rta isoform (i.e., despite being driven by different promoters, all MHV68 *Orf50* transcripts share the same ATG translation initiation codon located in the E1 exon and thus encode only a single isoform of RTA) (36). This, however, does not diminish the importance of additional promoters driving transcription since we have recently shown that it is the newly identified N4/N5 promoter that leads to the upregulation of *Orf50* transcripts during a helminth coinfection (39).

With the identification of newly discovered *Orf50* transcripts in the murine virus MHV68, we have expanded these studies to the human virus KSHV to determine whether these additional transcripts are conserved among other gammaherpesviruses. To investigate this, we performed 5′ RACE (rapid amplification of cDNA ends) analysis of RNA from BCBL-1 cells treated with 12-*O*-tetradecanoylphorbol-13-acetate (TPA). From this analysis, we were able to detect three previously unidentified gene 50 transcripts that initiated from two unique upstream promoters (Fig. 1B). We expanded these studies to primer walking in which a reverse primer was anchored in the E2 exon region and forward primers were used to walk up the region of the viral genome upstream Orf50. Primer walking confirmed the existence of the three additional transcripts that were identified through 5′ RACE analysis. It is important to note that the previously identified transcripts—E1-E2, E0A-E2, and E0B-E2—were also detected in our analysis. These analyses provided a more detailed picture of the KSHV *Orf50* transcription region.

In total, these analyses have identified six alternatively spliced RTA transcripts, driven from four distinct promoters (Fig. 1B). All of these transcripts ultimately splice to the major RTA coding exon, referred to as the E2 exon. The most proximal upstream

FIG 1 Legend (Continued)
a 2,728-bp intron and extending the E2 ORF by 7 amino acids, while generating RTA isoform 4. Green arrows denote short ATG-initiated ORFs that lie within the RTA transcripts. Of note is the ATG located within the E2 coding region that without splicing generates a nonfunctional RTA protein. Blue represents the coding region of each RTA isoform. The locations of the major ORFs antisense to gene 50 are also shown for reference.

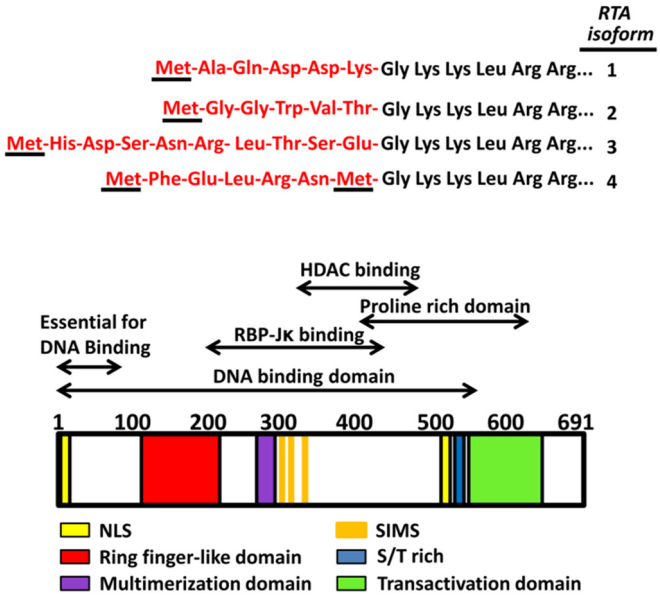

FIG 2 KSHV ORF50 alternative splicing leads to four RTA protein isoforms. (A) Amino acid structure of all four RTA protein isoforms. Black is representative of the homologous amino acid content of the exon 2 region, where for simplicity only the first 6 amino acids are shown. In red is the unique amino acid structure encoding each RTA isoform, isoform 1, a 6-amino-acid extension of the RTA protein generated by E1 and N4 transcripts; isoform 2, a 6-amino-acid extension of the RTA protein generated by E0A transcripts; isoform 3, a 10-amino-acid extension of the RTA protein generated by E0B transcripts; and isoform 4, a 7-amino-acid extension of the RTA protein generated by N5 transcripts. As seen, the small extensions of the RTA protein do not show any homologous amino acid content. (B) Various known functional domains of the RTA protein. Changes in amino acid structure by various isoforms only change a small number of amino acids but are changes to amino acids in the region essential for DNA binding. The essential DNA binding domains spans from amino acids 1 to 60, and the core DNA binding domain spans from amino acids 1 to 530. Also depicted are the ring finger-like domain (red), the multimerization domain (purple), the SUMO interaction motifs (SIMS) (orange), the serine/threonine-rich regions (blue), and the transactivation domain (green). Two nuclear localization signal sequences (NLS) are also depicted at the amino terminus end, as well as within the RTA protein toward the end of the DNA binding domain region (yellow). Also shown are the RBP-Jk and HDAC binding regions critical for RTA protein function.

initiated RTA transcript contains a 102-bp exon E1 exon, and its expression is driven from the proximal ORF50 promoter. The splicing of E1 to E2 results in the extension of ORF50, since there is an in-frame ATG located 18 bases from the 3′ end of E1 that encodes an additional 6 amino acids and generates RTA isoform 1 (Fig. 1B and 2A). The previously identified RTA proximal promoter lies upstream of the RTA distal promoter and drives the expression of two alternatively spliced transcripts containing either a short 234-base exon, E0A, which splices to the E2 exon removing a 1,901-bp intron, and a slightly longer 292-base exon, E0B, which splices to the E2 exon removing a 1,834-base intron (Fig. 1B). While being driven from the same promoter, the alternative splicing generated by E0A and E0B exons results in different extensions of the E2 ORF. The E0A extends the ORF by six unique amino acids, generating RTA isoform 2, while the E0B exon extends the ORF encoding a distinct amino terminus containing 10 amino acids, generating RTA isoform 3 (Fig. 2A). The next two identified transcripts are driven by the N3/N4 promoter (Fig. 1B). This promoter drives the expression of transcripts containing either a 857-base exon, N3, which splices to the E2 exon removing a 1,747-base intron while splicing to E2, or a 1,646-base exon, N4, which splices to the E2 exon (Fig. 1B). Notably, the N3 containing transcript does not result in the extension of the E2 ORF and thus is predicted to not result in the generation of a functional RTA protein. However, the N4 exon containing transcript shares the same 3′ sequences and splice donor with the E1 exon and thus is predicted to encode RTA isoform 1 (Fig. 2A). The last transcript identified is driven from the N5 promoter, which gives rise to a transcript containing a 351-base exon, N5, which splices out a large 2,728-base intron,

while splicing to E2 exon (Fig. 1B). The N5 exon contains an ATG that extends the E2 ORF by seven amino acids and results in the production of RTA isoform 4 (Fig. 2A). To date, there is no evidence that splicing to the E1 exon occurs (as is observed in MHV68) and, consistent with this, we have failed to identify a candidate splice acceptor in the region upstream of the E1 exon.

Characterization of the proximal, distal, N3/N4, and N5 promoters *in vitro*. With the identification of two previously unidentified promoters, as well as the lack of any characterization of the KSHV distal promoter, we investigated the activity of these candidate promoters. For all four promoters, 1,000-, 500-, 250-, and 100-bp promoter fragments were cloned into the pGL4.10 luciferase (pGL4.10[luc]) reporter vector. To first determine the minimal promoter region, we transfected the reporter vectors into the easily transfectable 293T cells (an embryonic kidney cell line). Luciferase assays confirmed that promoter activity was seen in all four Orf50 promoters, and we were also able to determine minimal promoter length, with the E1 promoter corresponding to a 250-bp fragment, whereas the E0A/B, N3/N4, and N5 promoters all corresponded to a 500-bp fragment directly upstream of the start of the exon (data not shown) Although 293T cells are easily transfectable, we wanted to determine the promoter activity of the Orf50 promoters in various cell types. All four different promoters, with constructs showing the greatest minimal promoter activity, were transfected into Vero (kidney epithelial), 3T12 (fibroblasts), and RAW 264.7 (macrophage) cells. These cell types were chosen since, unlike EBV, KSHV is able to initially infect epithelial cells, fibroblasts, and macrophages, in addition to lymphocytes. In addition, these cell types represent a much more uniform model of transfection for our luciferase expression system. The E1 promoter showed the greatest activity among all four promoters in Vero and RAW 264.7 cells, with ~5.7- and ~138-fold activities versus the empty vector (Fig. 3A). Interestingly, the N3/N4 promoter showed the greatest activity, an ~55.5-fold change over empty vector in 3T12 cells (Fig. 3C). This is intriguing because the N3/N4 promoter generates the N4 transcript, which encodes the same RTA isoform 1 as the E1 promoter (Fig. 1B and 2A). The N5 promoter showed modest activity in all three cell lines compared to the E1 or N3/N4 promoter, with an ~2.2-fold increase in Vero cells, an ~11.72-fold increase in 3T12 cells, and an ~31.67-fold increase in RAW 264.7 cells in relation to the empty expression vector control plasmid (Fig. 3D). The least active promoter was the E0 promoter, which is interesting because it drives transcripts that encode two unique RTA isoforms, 2 and 3 (Fig. 1B and 2A). The E0 promoter showed almost no promoter activity in all cell types tested (Fig. 3B). This could indicate that these transcripts are rare or that the activation of this promoter requires a specific cellular environment or cellular stimulation. One such stimulation is potentially RTA isoforms themselves, as described below. Alternatively, it is possible that there is a distal enhancer element in the viral genome that contributes to the expression of some (or all) of the RTA isoforms.

KSHV RTA isoforms exhibit distinct patterns of viral promoter activation. While promoter activity was observed for all four Orf50 promoters in a variety of cell lines, one of the most critical functions of the RTA protein is to act as a transcriptional activator of downstream viral genes. As previously noted (18, 40), the proximal Orf50 promoter-driven E1-E2 transcript results in the significant extension of the Orf50 open reading frame, which is critical for the transactivation potential of RTA (Fig. 2B). RTA isoform 1 is 691 amino acids in length and has been noted to contain several different domains that are critical for its function (Fig. 2B) (41–43). One of the critical functions lies in the amino terminus of the protein, in which the first 60 amino acids play an important role in transcriptional activation and the ability of the RTA protein to bind to target viral and cellular promoters. Indeed, it is precisely this region that may be impacted by having unique amino-terminal sequences in the newly identified RTA isoforms (Fig. 2A). For this reason, we assessed the transactivation potential of the identified RTA isoforms, comparing their function to the well-characterized RTA isoform 1, which has been shown to transactivate many viral promoters (32).

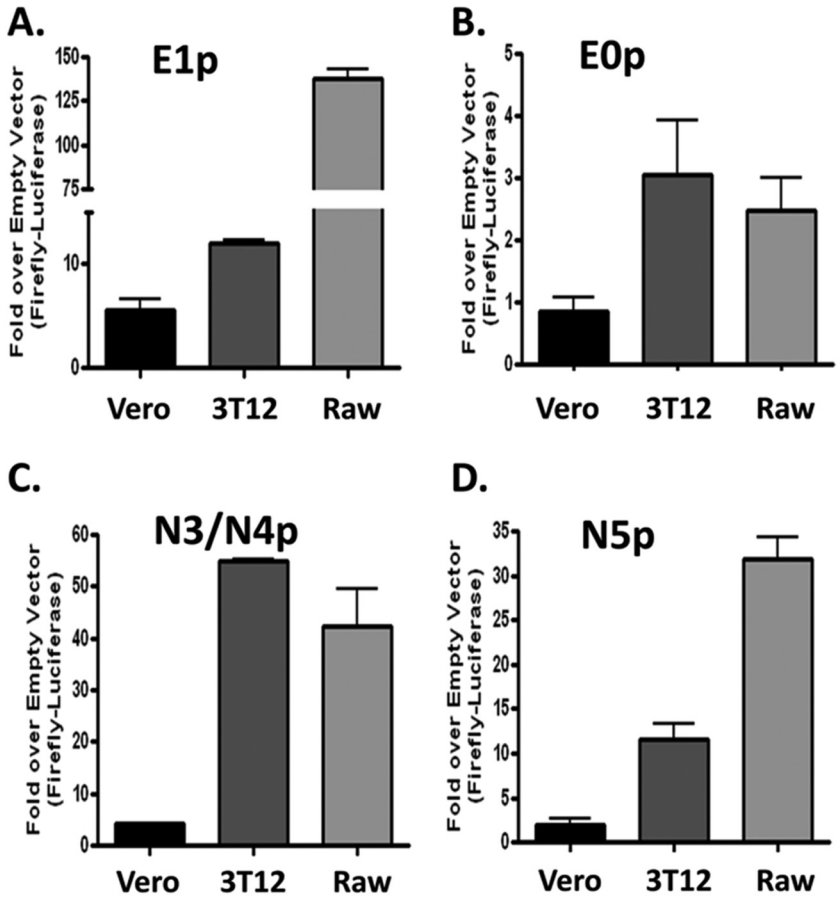

FIG 3 Promoter activity of the proximal, distal, N3/N4, and N5 Orf50 KSHV promoters in various cell types. (A) Vero, 3T12, and RAW 264.7 cells were transfected with pGL4.10[luc] luciferase reporter construct containing 250 bp upstream of the E1 exon. At 48 h posttransfection, luciferase assays were performed. (B) Vero, 3T12, and RAW 264.7 cells were transfected with the pGL4.10[luc] luciferase reporter construct containing 500 bp upstream of the E0A and E0B exon. At 48 h posttransfection, luciferase assays were performed. (C) Vero, 3T12, and RAW 264.7 cells were transfected with the pGL4.10[luc] luciferase reporter construct containing 500 bp upstream of the N3 and N4 exon. At 48 h posttransfection, luciferase assays were performed. (D) Vero, 3T12, and RAW 264.7 cells were transfected with the pGL4.10[luc] luciferase reporter construct containing 500 bp upstream of the N5 exon. At 48 h posttransfection, luciferase assays were performed. Data are presented as the fold difference in firefly luciferase activity versus the pGL4.10 empty vector control. The data represent triplicates of at least three independent transfections.

For this analysis, we cloned each RTA isoform into a pCMV-Flag2B expression vector. To ensure that each RTA isoform was efficiently expressed, immunoblots were performed at 48 h posttransfection of 293T cells and probed with an anti-FLAG antibody for the expression levels of each RTA isoform (Fig. 4). Although some variation in the

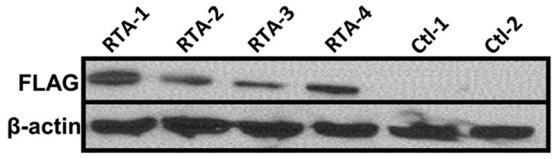

FIG 4 Immunoblot analyses of RTA isoform protein expression levels in transfected 293T human embryonic kidney cells. 293T cells were transfected with 2.5 μg of pCMV-Flag2B-Iso1, pCMV-Flag2B-Iso2, pCMV-Flag2B-Iso3, and pCMV-Flag2B-Iso4 DNA. For an expression control, cells were transfected with 2.5 μg of pCMV-Flag2B-Empty Vector (Ctl-1), and for a transfection control, cells were mock transfected (Ctl-2). The cells were harvested at 24 and 48 h posttransfection and lysed, and 30 μg of protein was used for the immunoblot analyses to assess the RTA expression levels. FLAG expression was used as readout of RTA protein expression from the pCMV-Flag2B vector. Immunoblots were stripped and then reprobed for β-actin levels to ensure equal protein loading.

levels of the RTA isoforms was detected (this was variable between experiments, suggesting that it may be related to transfection efficiency), we consistently detected robust expression of each RTA isoform. To ensure equal protein loading, β-actin was used as an internal control (Fig. 4).

To assess activation of viral genes by each RTA isoform, a library of KSHV ORF promoter sequences was cloned into luciferase reporter constructs. The majority of these constructs were recreated from a promoter library provided by Y. Izumiya (32). The promoter sequence was recapitulated from historical data and, if historical data were unavailable, 1,000-bp promoter fragments immediately upstream of the ORF were used. 293T cells were transfected with the various KSHV promoter reporter constructs, along with either an empty vector expression construct or a construct containing either isoform 1, 2, 3, or 4 RTA. After 48 h, the cells were harvested, and luciferase assays were performed. Data were generated in triplicate and plotted as the fold change caused by the expression of an RTA isoform versus the basal activity of a promoter when expressed with empty vector control. The compiled data from these analyses is depicted as the transactivation of individual KSHV promoters by each RTA isoform relative to the activity of RTA isoform 1 (Fig. 5) and as a heat map showing the fold RTA isoform transactivation of each KSHV promoter (Fig. 6).

From this analysis it is clear that all of the identified RTA isoforms retain the ability to transactivate numerous KSHV viral promoters (Fig. 5 and 6). With respect to the heat map shown in Fig. 6, viral promoters were ordered from highest to lowest transactivation by RTA isoform 1. Notably, each RTA isoform exhibits a distinct pattern of viral gene activation, with RTA isoforms 2 and 4 strongly activating a smaller subset of KSHV promoters compared to RTA isoform 1 (Fig. 6). In contrast, RTA isoform 3 was a relatively weak activator of KSHV promoters (Fig. 6). Overall, we observed that RTA isoform 1 was the strongest transactivator, but there were exceptions; e.g., the Orf6 promoter activated by isoform 2, the K3 promoter activated by isoform 4, and the K4 promoter activated by both isoforms 2 and 3 were all stronger than isoform 1 (Fig. 5). Despite these exceptions, when the overall pattern of RTA isoform transactivation was examined, a pattern of decreasing transactivation potential emerged (Fig. 6 and Table 1). Of the 86 promoters tested, RTA isoform 1 has the ability to transactivate 72% of the promoters $>$10-fold. This pattern is reversed for RTA isoform 4, where 78% of the promoters tested resulted in $<$10-fold activation (Table 1 and Fig. 6).

One important aspect of RTA function is its ability to upregulate its own expression. Although previously the only known RTA isoform was RTA isoform 1, it is now important to determine the pattern that emerges when each isoform is used in conjunction with the newly discovered promoters associated with driving the expression of the different RTA isoforms. Importantly, the distal Orf50 promoter is most strongly activated by the RTA isoforms, with isoform 1 activating it $>$100-fold, followed by isoforms 2, 3, and 4 activating this promoter $>$25-fold. The most distal Orf50 promoter, N5, is the next most strongly activated, with isoforms 1 and 4 activating it $>$25-fold, while isoforms 2 and 3 activate it $<$10-fold. The Orf50 proximal promoter (driving isoform 1 expression) is autoactivated by isoform 1 $>$25-fold, whereas it is only activated $<$10-fold by the other RTA isoforms. Finally, the Orf50 N3 promoter is weakly activated $<$10-fold by all of the RTA isoforms. Thus, from this analysis we predict that transcription of Orf50 from the proximal promoter (leading to the expression of RTA isoform 1) is quickly followed by upregulation of the more distal Orf50 promoters, leading to the expression of RTA isoforms with more limited/focused transactivation of downstream KSHV genes. Based on other viral and cellular genes driven by multiple promoters, it is likely that upstream transcription initiation will suppress transcription initiation at the more proximal Orf50 promoter through transcription interference (44, 45). Finally, it is important that without RTA expression the distal promoter Orf50 promoter is very weak and, as such, it is likely that the initial expression of isoform 1 and/or isoform 4 is required for the efficient expression of RTA isoforms 2 and 3 (Fig. 3B).

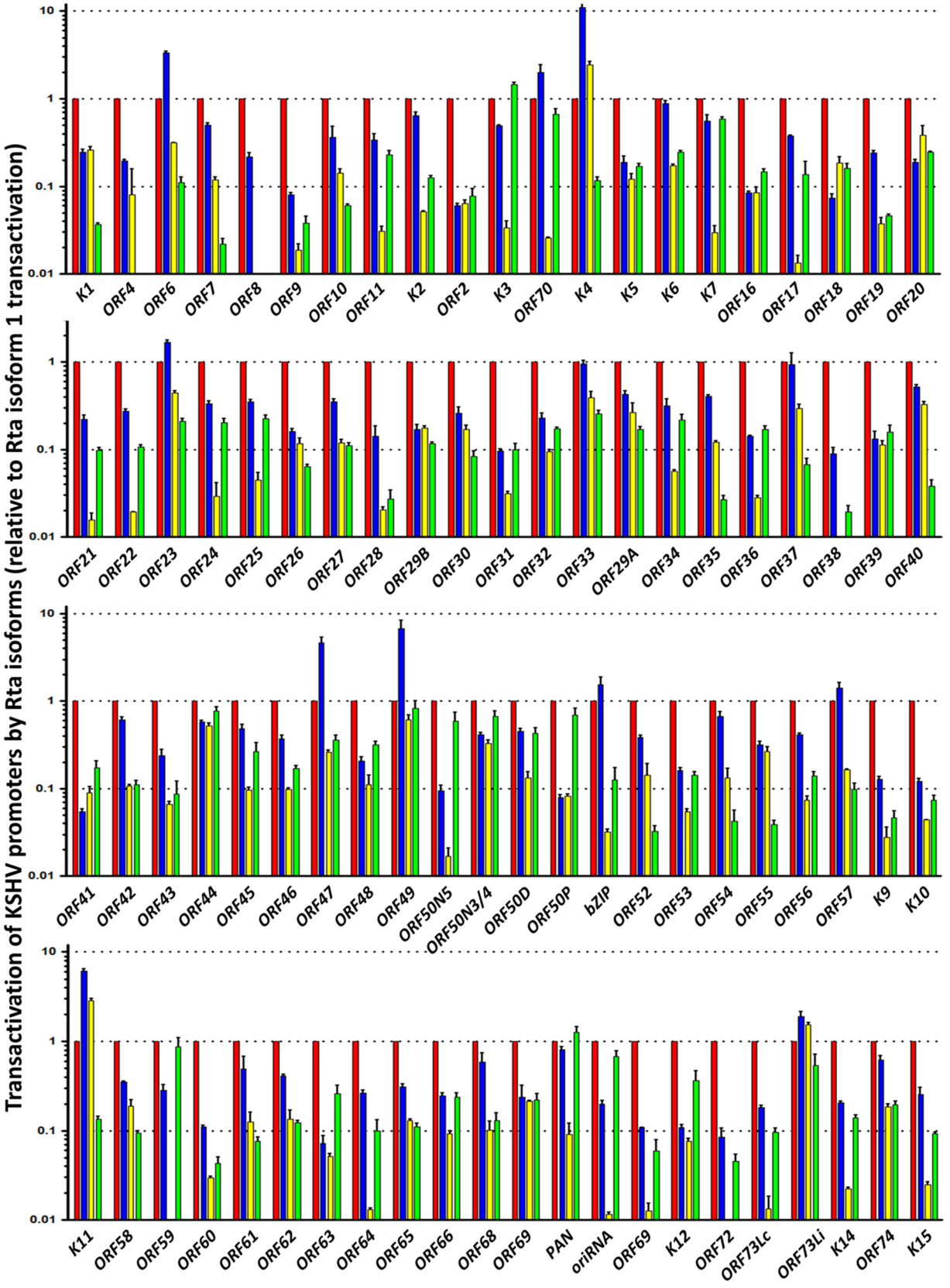

FIG 5 Transactivation potential of newly identified isoforms 2 to 4 compared to the transactivation potential of isoform 1 in 293T cells. Data generated from the transfection and transactivation experiment are plotted as the fold change in promoter transactivation potential compared to isoform 1, with isoform 1 set to 1. Experiments were conducted in triplicate, and data are plotted as the averages of three experiments. Isoform 1 is shown in red, isoform 2 is shown in blue, isoform 3 is shown in yellow, and isoform 4 is shown in green. The viral ORFs are shown in order

(Continued on next page)

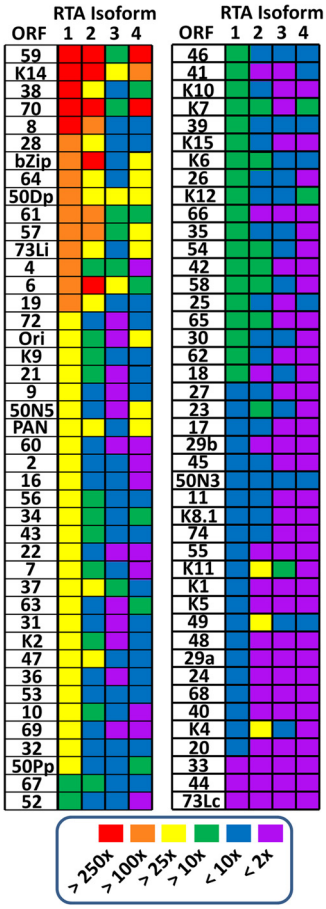

FIG 6 Transactivation potential for all RTA isoforms, where the general fold change in the activation of promoters associated with viral ORFs is shown. 293T cells were transfected with RTA isoform expression constructs in conjunction with promoter luciferase constructs for each viral ORF. Viral ORFs are grouped into six categories based on the fold change over the expression of empty vector and the absence of RTA protein; these categories are >250-fold (red), >100-fold (orange), >25-fold (yellow), >10-fold (green), <10-fold (blue), and <2-fold (purple). ORFs are shown in the order from most transactivated by isoform 1 to least transactivated by isoform 1. There are five columns, with the first column depicting the viral ORF promoter, and the next four columns depicting the expression of isoforms 1, 2, 3, and 4. All experiments were performed in triplicate, and the results are shown as an average of these experiments.

The presence of other viral proteins does not alter RTA isoform transactivation of two representative KSHV promoters. Although RTA can transactivate many viral genes, it also contains a number of protein-protein interaction domains (Fig. 2B). These domains allow RTA to work in tandem with other cellular and viral proteins, such as b-ZIP, to facilitate virus replication (32, 46, 47). Although the complexity of these interactions is beyond the scope of the present study, we wanted to determine whether the presence of other viral proteins changed the transactivation potential of RTA isoforms. We utilized the 293TΔ50BAC cell line, which harbors a latent KSHV genome lacking a functional Orf50, to assess the impact of RTA isoforms 1 and 4 on two target KSHV promoters: the KSHV bZIP and PAN promoters. Notably, we chose these promoters based on our analyses of RTA isoform transactivation in 293T cells, where we observed a large difference in RTA isoforms 1 and 4 transactivation of the bZIP promoter (>100-fold versus >25-fold, respectively) (Fig. 6). In contrast, similar levels of PAN promoter activation were observed with RTA isoforms 1 and 4 (both >25-fold in

FIG 5 Legend (Continued)
of their location within the KSHV genome. ORFs that do not contain a bar corresponding to a given isoform are isoforms with transactivation differences below the given cut off 0.01 (e.g., Orf38 and Iso3).

TABLE 1 Summary of the fold induction of KSHV promoters by each RTA isoform

	No. of promoter samples			
Fold induction	**RTA-1**	**RTA-2**	**RTA-3**	**RTA-4**
>250	5	5	0	2
>100	10	3	0	1
>25	26	12	3	8
>10	21	18	6	8
<10	21	32	37	27
<2	3	16	40	40

293T cells) (Fig. 6). When isoform 1 RTA was expressed in the presence of the bZIP promoter in the 293TΔ50BAC cell line, we observed a transactivation pattern similar to that seen in 293T cells (Fig. 7A). To ensure the good expression of other viral proteins in conjunction with RTA isoform expression, we also treated the 293TΔ50BAC cells with phorbol ester (TPA). Importantly, the addition of TPA did not alter the observed levels of either RTA isoform 1 or 4 transactivation of the bZIP promoter (Fig. 7A). Overall, the results with RTA isoform transactivation of the bZIP promoter in the 293TΔ50BAC cell

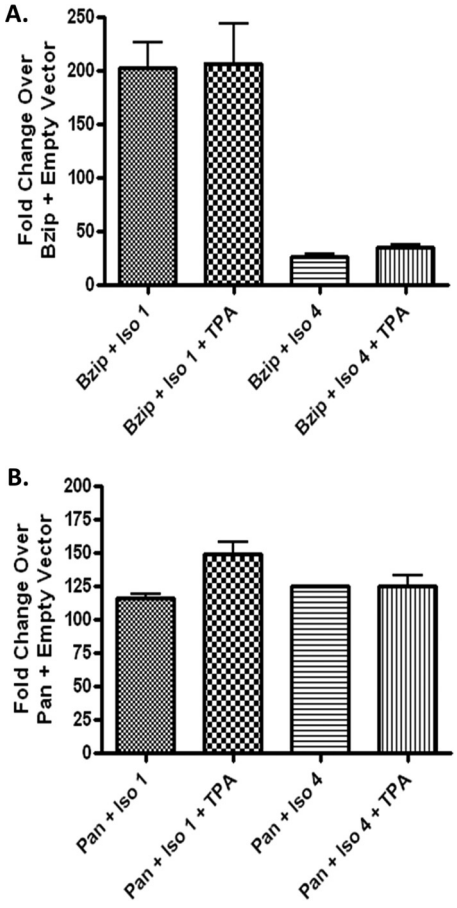

FIG 7 Promoter activity of K-bZIP and PAN when transfected in the presence of RTA isoform 1 or 4, as well as the potential expression of other viral proteins. (A) 293TΔ50BAC cells, containing all other viral proteins but RTA, were transfected with 1.25 μg of K-bZIP pGL4.10[luc] luciferase reporter constructs in conjunction with 1.25 μg of pCMV-Flag2B-Iso1 or pCMV-Flag2B-Iso4. The cells were left either untreated or stimulated with TPA and, at 48 h after transfection, luciferase assays were performed. (B) 293TΔ50BAC cells were transfected with 1.25 μg of PAN pGL4.10[luc] luciferase reporter constructs in conjunction with 1.25 μg of pCMV-Flag2B-Iso1 or pCMV-Flag2B-Iso4. These cells were also left either untreated or stimulated with TPA and, at 48 h after transfection, luciferase assays were performed. Data are presented as the fold change versus the reporter construct plus pCMV-Flag2B-Empty Vector. The data represent triplicates of at least three independent transfections.

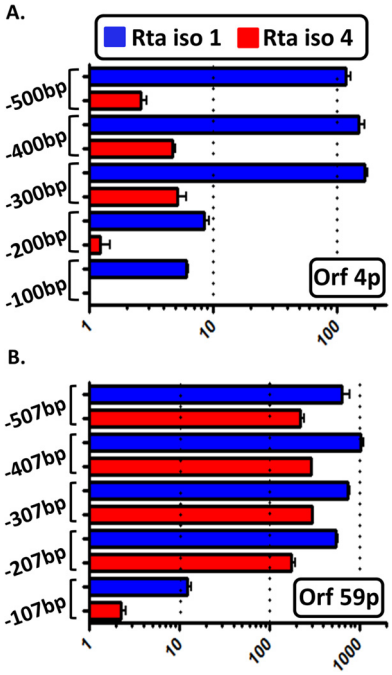

FIG 8 RTA isoforms have the potential to share a RRE binding site. (A and B) Reporter constructs were generated for both the Orf4 and the Orf59 KSHV promoters. We generated 100-bp deletions starting in the context of 507 bp (Orf59) and 500 bp (Orf4) and cloned them into the pGL4.10[luc] luciferase reporter construct. 293T cells were transfected with the reporter constructs in conjunction with the expression constructs pCMV-Flag2B-Iso1 or pCMV-Flag2B-Iso4. At 48 h posttransfection, luciferase assays were performed. Data are plotted as fold changes versus empty vector on a log scale. Experiments were performed in triplicate, and graphs depict the average.

line closely recapitulated the results obtained in 293T cells. We extended these analyses to assessing the PAN promoter, which is equivalently activated by both RTA isoforms 1 and 4 in the 293T cell line (Fig. 5 and 6). In the 293TΔ50BAC cell line we observed that both RTA isoforms 1 and 4 resulted in similar levels of transactivation observed in 293T cells, both with and without TPA induction (Fig. 7B). Although we cannot rule out an effect of additional viral proteins on the ability of RTA isoforms to transactivate viral promoters, these experiments indicate that the differences observed in the transactivation potential of the newly identified RTA isoforms is not rescued by the expression of other viral (or cellular) proteins induced during the lytic cycle. However, this could be different for other viral and/or cellular promoters targeted by RTA.

Newly identified RTA isoforms appear in some, but not all, viral promoters to utilize the same RTA response elements. Although there is little consensus on what defines an RTA response element (RRE) within the KSHV genome, we attempted to determine whether the newly identified RTA isoforms share RREs or whether they bind to previously unidentified RRE sites. To do this, we utilized promoter luciferase constructs for both Orf59 and Orf4. Orf59 was chosen because it represents the highest fold change in promoter activity for both RTA isoforms 1 and 4 (>250-fold) (Fig. 6). Orf4 was chosen because it represents a promoter that is strongly activated by RTA isoform 1, resulting in a >100-fold increase in promoter activity, whereas in comparison RTA isoform 4 does not significantly transactivate the Orf4 promoter (<2-fold in 293T cells) (Fig. 6). To begin to assess whether RRE sites are shared between the different RTA isoforms, we created 100-bp truncations of the Orf59 or Orf4 promoter starting at the promoter sequence previously defined (bp −507 for Orf59 and bp −500 for Orf4) (32, 48). When we look at Orf59 promoter activation, we observed an ~650-fold activation in the presence of RTA isoform 1 and an ~225-fold activation in the presence of RTA isoform 4 (Fig. 8B). Deleting the upstream sequences to bp −207 had no significant impact on either RTA isoform 1 or isoform 4 activation of the Orf59 promoter. However,

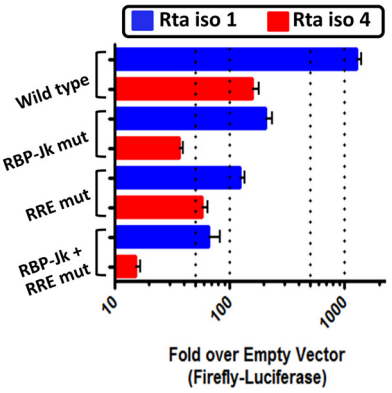

FIG 9 RTA isoforms can interact with cellular transcription factors in a synergistic manner. Reporter constructs were generated for the Orf57 KSHV promoter. Four constructs were generated: a full-length Orf57 KSHV promoter, an RTA responsive element (RRE) deletion in the context of the Orf57 KSHV promoter, an RBP-Jk deletion in the context of the Orf57 KSHV promoter, and an RRE plus RBP-Jk deletion in the context of the Orf57 KSHV promoter. All constructs were cloned into the pGL4.10[luc] luciferase reporter and transfected in conjunction with pCMV-Flag2B-Iso1 or pCMV-Flag2B-Iso4 into 293T cells. At 48 h posttransfection, luciferase assays were performed. Data are presented as the fold difference versus the expression construct plus the pCMV-Flag2B-Empty Vector. The data represent triplicates of at least three independent experiments.

deletion of sequences from bp −207 to bp −107 dramatically decreased the RTA isoform 1 and 4 activation (by ~12- and ~2-fold, respectively) (Fig. 8B). These results indicate that isoforms 4 and 1 likely share an RRE site, although fine-mapping studies are required to confirm this prediction.

To further explore this issue, we examined the Orf4 promoter, which is not significantly activated by RTA isoform 4 (Fig. 6). When the bp −500 Orf4 promoter fragment was assayed, we observed ~116-fold activation by RTA isoform 1 but <3-fold activation by RTA isoform 4 (Fig. 8A). The weak activation of the Orf4 promoter by RTA isoform 4 was observed with all the Orf4 promoter truncations used (Fig. 8A). RTA isoform 1 activation of the Orf4 promoter was dramatically reduced by a deletion that removed promoter sequences upstream of bp −200 (a decrease from ~169- to ~8-fold activation) (Fig. 8A). This decrease indicates that the isoform 1 RRE site(s) map in the region from bp −200 to bp −300. Analysis of the Orf4 promoter demonstrates that there exist RRE elements that are selectively used by the different RTA isoforms. Further mapping and characterization of these *cis* elements is required to determine the basis for this selectivity.

To further characterize RTA isoform 1 and 4 activation, we assessed the activation of the well-characterized Orf57 promoter that contains defined RRE and RBP-Jk sites that functionally synergize (49–51). The Orf57 promoter is appropriate for assessing the role of the defined RRE and RBP-Jk sites since it is strongly activated by both RTA isoforms 1 and 4 (Fig. 5 and 6). First, we determined the baseline level of RTA upregulation for both isoforms 1 and 4 and observed that RTA isoform 1 resulted in an ~1,260-fold increase in Orf57 promoter activity and that isoform 4 RTA resulted in an ~170-fold increase in promoter activity (Fig. 9). Since RTA has been shown to interact with RBP-Jk to increase promoter activity (51), we next generated an RBP-Jk binding mutant within the context of the Orf57 promoter. When the RBP-Jk binding site was mutated, the activation of promoter activity in the presence of isoform 1 RTA dropped to ~210-fold, while in the presence of isoform 4 RTA it dropped to ~42-fold (6- and 4-fold decrease in activation, respectively) (Fig. 9). We next sought to determine whether both RTA isoforms 1 and 4 shared the consensus Orf57 RRE site by mutating the known RRE site in the context of the Orf57 promoter. The mutation of the RRE site decreased RTA isoform 1 activation by ~120-fold (a 10.5-fold decrease in activity compared to the intact promoter) and RTA isoform 4 activation by ~50-fold (a 3.5-fold decrease in activity compared to the intact promoter) (Fig. 9).

Finally, we mutated both the RRE and the RBP-Jk sites. The double mutant was activated ~65-fold by RTA isoform 1 and ~15 by RTA isoform 4 (a 19-fold decrease in RTA isoform 1 activation and an 11-fold decrease in RTA isoform 4 activation) (Fig. 9). The residual activation observed with both isoforms indicates the presence of additional *cis* elements within the Orf57 promoter that can mediate RTA activation. Whether the difference in the magnitude of RTA isoform 1 and 4 activation of the Orf57 promoter reflects different affinities of these isoforms at the same *cis* elements or the presence of *cis* elements that selectively interact with RTA isoform 1 and not RTA isoform 4 remains to be determined. However, this analysis does provide direct evidence that both RTA isoforms 1 and 4 can synergize with RBP-Jk and that they can function through a common RRE within the Orf57 promoter.

RTA isoforms with lower transactivation potential do not significantly interfere with RTA isoform 1 transcriptional activation. Finally, since RTA functions as a dimer (41), we investigated whether the expression of RTA isoforms with lower transactivation potential could attenuate transcriptional activation mediated by RTA isoform 1. If so, this could be an additional mechanism for modulating RTA activity. To assess this, we chose two KSHV promoters, one of which is strongly activated by RTA isoform 1 (Orf28 promoter) and one which is more modestly transactivated by RTA isoform 1 (Orf60), but both of which are only weakly activated by the other RTA isoforms (see Fig. 5 and 6). In each case, we assessed the transactivation of the target promoter by the RTA isoforms alone, as well as titrating in increasing amounts of expression vector (0.25 to 1 μg of DNA) for each isoform (holding consistent the total amount of expression plasmid transfected, using empty expression plasmid in conjunction with that encoding each RTA isoform) in the presence of a fixed amount of RTA isoform 1 (0.5 μg of DNA) expression plasmid (Fig. 10). RTA isoform 2 appeared to weakly augment the RTA isoform 1 activation of both the Orf28 and Orf60 promoters, whereas RTA isoforms 3 and 4 weakly inhibited RTA isoform 1 transactivation of the Orf28 promoter (but not the Orf60 promoter) (Fig. 10). The failure to observe significant attenuation of RTA isoform 1 activation upon expression of another RTA isoform with less transactivation potential suggests (i) that these isoforms do not heterodimerize with RTA isoform 1 and that they do not efficiently compete for RTA isoform 1 binding at the Orf28 or Orf60 promoters and/or (ii) that they are able to heterodimerize with RTA isoform 1 but that these heterodimers exhibit the same transcriptional activation potential as RTA isoform 1 homodimers. The weak inhibition of RTA isoform 1 transactivation of the Orf28 promoter by RTA isoforms 3 and 4, observed when much higher levels of RTA isoform 3 and 4 expression plasmids were transfected into cells, would be consistent with inefficient competition of these isoforms with RTA isoform 1 for binding to the relevant RRE(s) in this promoter.

DISCUSSION

We demonstrate here that KSHV gene 50 transcription is more complex than previously described and that it is very similar to the pattern of gene 50 transcription in the rodent gammaherpesvirus MHV68 (35, 36). Based on the current analysis, KSHV RTA expression can be driven from four distinct promoters, resulting in the expression of six distinct alternatively spliced gene 50 transcripts. Unique to KSHV gene 50 transcription is that these six different spliced gene 50 transcripts encode several isoforms of RTA. The identification of multiple promoters driving expression of a single gene is not novel to the KSHV *Orf50* gene (52–55). Even within the gammaherpesvirus family, the expression of genes other than Orf50 is driven by multiple promoters, resulting in differential splicing; EBV uses this process to encode six EBNA gene products (56–60). The use of multiple promoters to drive expression of a critical factor in the gammaherpesvirus life cycle points to the likely complexity involved in controlling acute replication, latency, and reactivation. Multiple promoters may confer the ability of the virus to respond to an array of external stimuli, as well as offering a mechanism to modulate viral gene expression through the expression of different

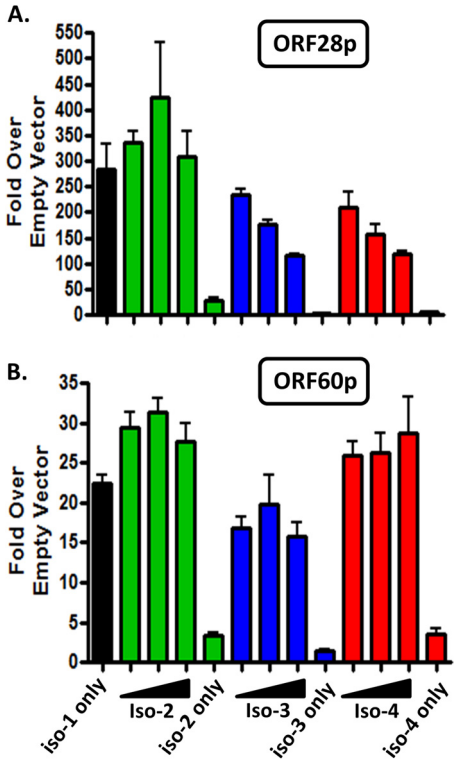

FIG 10 Characterization of RTA isoform 1 transactivation of target KSHV promoters in the presence of the other RTA isoforms. We analyzed RTA isoform 1 transactivation of the Orf28 promoter (A) and the Orf60 promoter (B) in the absence or presence of increasing levels of different RTA isoforms. 293T cells were transfected with a steady dose of both isoform 1 RTA and reporter construct. As indicated, increasing doses of isoform 2 (green), isoform 3 (blue), and isoform 4 (red) were cotransfected with isoform 1, and the transactivation potential of isoform 1 was determined. The single transactivation potential of isoforms 1, 2, 3, and 4 was also determined as a control. Data are plotted in triplicate, and graphs represent the average fold change versus the empty vector control.

protein isoforms coupled with transcriptional interference mediated by upstream transcription initiation (60, 61).

What is unique to KSHV Orf50 is that four different isoforms of RTA are generated by the use of multiple promoters, differing from MHV68 in that multiple promoters drive one single isoform of RTA. This raises the question of why KSHV encodes different isoforms of RTA while its genetically similar cousin MHV68 fails to do so? There are many possible explanations; one possible explanation is that KSHV has evolved different RTA isoforms to deal with a different life cycle than what is found in MHV68. KSHV and its ability to lead to the formation of KS tumors is highly unique, indicating passage into different cell types. A second and perhaps more likely possibility is that we have simply failed to identify RTA isoforms that occur in MHV68. For example, the E0 exon in MHV68 may bypass the E1 exon and splice directly to the E2 exon. If this were to occur, an in-frame extension of the E2 ORF would occur, and a new RTA isoform in MHV68 would be generated.

To begin to address the role multiple Orf50 promoters might play during KSHV infection, we assessed the basal activity of these promoter is several cell lines. Although it appears that all of the identified Orf50 promoters have basal activity in these cell lines assayed, several of the promoters exhibited variable activity depending on the cell line tested (Fig. 3). The E1/proximal promoter exhibited significant activity above the empty vector control, with the highest activity observed in RAW 264.7 cells, a macrophage cell line. The N3/N4 promoter also exhibited significant basal activity above the empty vector control, with the highest activity observed in NIH 3T12 and RAW 264.7 cells. It is interesting that the two promoters with the highest levels of basal activity in the

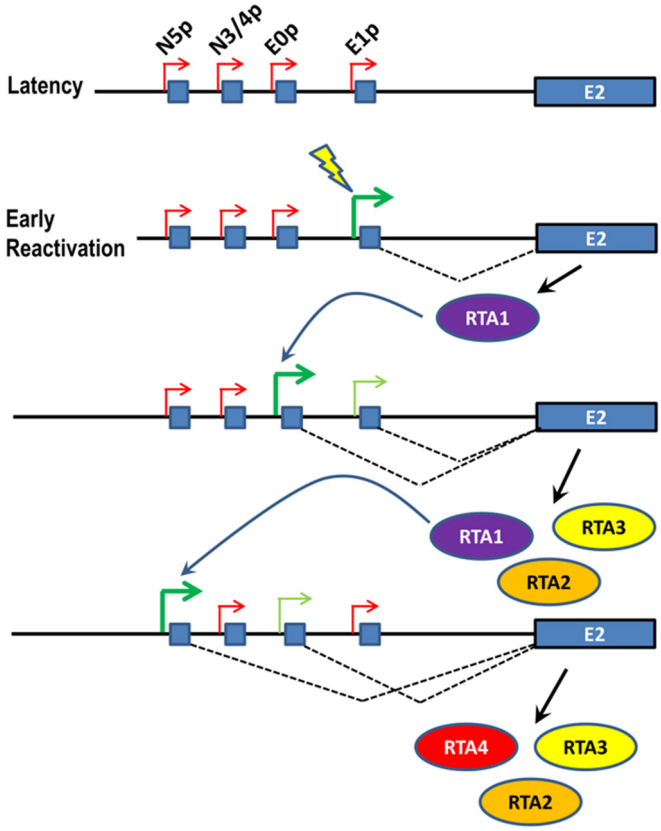

FIG 11 General model showing how transcriptional interference mediated by upstream Orf50 transcription initiation, combined with the expression of different RTA isoforms, may modulate the cascade of KSHV lytic gene expression.

three cell lines tested encode RTA isoform 1. The E1/proximal promoter drives expression of the E1-E2 spliced transcript, while the N3/N4 promoter results in the N4-E2 spliced transcript, with both of these transcripts sharing a splice donor site (i.e., the N4 exon is a 1,544-base extension of the E1 exon that does not alter the RTA coding sequence) (Fig. 1B). This suggests that the dominant isoform of RTA, at least early in virus replication, is isoform 1 and that isoforms 2, 3, and 4 are required for more subtle regulation of viral transactivation (consistent with the more restricted pattern of viral gene activation exhibited by these RTA isoforms). It is also interesting that the E0/distal promoter had almost undetectable levels of basal activity in all three cell types tested (Fig. 3B). The E0/distal promoter drives the transcription of two of the four RTA isoforms, RTA isoforms 2 and 3. Tight regulation of isoforms 2 and 3 is consistent with a unique role these RTA isoforms may play within the viral life cycle. In addition, it is important to note that whereas the E0/distal promoter exhibited very low basal activity, it was the Orf50 promoter most strongly activated by all the RTA isoforms (Fig. 6). Taken together, these findings support a model in which the expression of RTA isoforms 2 and 3 is only induced after the expression of RTA isoform 1. A general model of how alternative transcription initiation and alternative RTA isoform expression may arise is presented in Fig. 11. In this model, we hypothesize that reactivation from latency requires an initial stimulus that drives activation of the Orf50 E1/proximal promoter, leading to expression of RTA isoform 1. This in turn activates transcription initiation from the E0/distal promoter, leading to the expression of isoforms 2 and 3, and then induction of the N5 promoter, leading to the expression of RTA isoform 4. Ultimately, the induction of upstream Orf50 promoter activity suppresses (through transcriptional interference) transcription initiation at the more the proximal Orf50 promoters, ultimately quelling the expression of RTA isoform 1. Notably, transcriptional interference

also plays an important role in regulating EBV gene expression (60–63). Further experiments will be conducted to determine the time course of *Orf50* transcript generation and promoter usage during the course of a primary infection, as well as reactivation from latency. The difficulties of these experiments cannot be understated and represent the next step in the evolution of this project. Most likely, many different factors go into promoter usage, and even a general experiment such as TPA reactivation of PEL cell lines will not represent what most likely is a very complex and well-regulated system during the course of a natural infection.

Importantly, in the model shown in Fig. 11, we have not depicted activity from the N3/N4 promoter, based on our observation that this promoter is only weakly activated by the various RTA isoforms. We predict that either this promoter may play a role in the initial expression of RTA isoform 1 during reactivation or in permissive cells (not depicted in our model) and/or that it has evolved to play a highly specialized role during infection, perhaps being responsive to specific signals (e.g., inflammatory signals [see further discussion below]).

Although the basal activity of the Orf50 promoter-driven reporter constructs in various cell lines is informative, it does not take into account the impact that epigenetic modifications of the viral genome may play in the usage of these promoters *in vivo*. For example, additional experiments need to be conducted to determine the methylation status of the newly identified promoters, as we have previously done for MHV68, although a suitable *in vivo* model still does not exist. Furthermore, the assessment of basal Orf50 promoter activity was carried out in cell lines that are permissive for MHV68 replication. Regulation of the Orf50 promoters in cell types that are sites for the establishment of latency is likely to be different. In addition, these studies have not assessed how responsive the Orf50 promoters are to various stimuli (e.g., those that modulate B cell function). It has been clearly shown that gammaherpesviruses respond to many outside stimuli, one being gamma interferon (IFN-γ), which has been shown to suppress Orf50 promoter activity (64–68). Not only has Orf50 transcription been shown to be responsive to IFN-γ, but also a recent study has shown that a helminth coinfection of MHV68 latently infected mice can lead to viral reactivation (39). The latter is mediated through the action of the cytokine IL-4, which is produced in large quantities during helminth infection and is able to overcome IFN-γ repression of Orf50 transcription, specifically upregulating transcription from one of the newly identified MHV68 Orf50 promoters, the N4/5 promoter (39). This example illustrates the importance of multiple promoters, where in MHV68 only one of the four promoters is able to respond to a coinfection environment triggering reactivation from latency.

While the external cellular environment is important, so is the internal environment within each individual infected cell, where transcription factors such as XBP-1 binding viral promoters can alter the viral life cycle (69–72). One of the most important functions of RTA is the ability to initiate a downstream cascade of viral gene expression. RTA does this by binding to various viral promoters and inducing gene transcription (26, 27, 32, 73). Although this ability to act as a transcriptional activator has only been characterized with RTA isoform 1, it begs the question as to whether the newly identified RTA isoforms work in a similar manner to generate a cascade of gene transcription. While the RTA isoforms only differ by a short sequence at their amino termini, this region of RTA is known to be important for function (Fig. 2) (18, 24). As shown here, altering a short sequence at the amino terminus of RTA indeed has a major impact on RTA-mediated activation of KSHV genes (and, presumably, on cellular genes as well, although we did not assess this) (see Fig. 5 and 6).

Although our working model is supported by what we observed, there are caveats to this hypothesis. First, as mentioned previously, the promoters themselves may respond to different external stimuli, resulting in the upregulation of a particular RTA isoform. Second, whereas RTA isoform 1 is overall the most potent transcriptional activator of KSHV gene transcription, there are exceptions with respect to the specific KSHV promoter. For example, we observed that the Orf6, K3, Orf70, K4, Orf23, Orf33,

Orf37, Orf47, Orf49, bZIP, Orf57, K11, PAN, K12, and Orf73Li promoters can all be transactivated better by an RTA isoform other than isoform 1 (Fig. 5 and 6). It is interesting to speculate that the altered spectrum of KSHV gene activation by the RTA isoforms might play a role in driving some virus-infected cells toward establishing a latent infection. For example, K12 is the transcript most abundantly generated during KSHV latency, and therefore its greater upregulation may point toward the ability of isoform 4 RTA to impact the switch to viral latency (74, 75). Another interesting promoter is the Orf73Li promoter that drives the transcription of the latency-associated protein LANA. This protein is essential for the establishment, maintenance, and control of viral latency (76–80). Two other unique transcripts that are more strongly upregulated by RTA isoform 2 than RTA isoform 1 are the Orf47 and Orf49 promoters, which drive the expression of transcription that are antisense to the Orf50 region (Fig. 1B and 5). The upregulation of antisense transcripts adds another layer of possible transcriptional control for the Orf50 region, since antisense transcripts have been associated with a silencing of transcription on the sense strand (81, 82).

Another factor that may play a role in the RTA isoform's ability to transactivate promoters is the ability to interact with other viral proteins and transcription factors. Although only a small portion of the N-terminal end is changed, leaving the protein binding domain as well as other important RTA functional domains intact (Fig. 2B), we wanted to determine whether the presence of other viral proteins affected the ability of the RTA isoforms to transactivate viral promoters. For example, the presence of k-bZIP is known to associate with isoform 1 RTA to aid in the upregulation of several viral promoters (32, 47). Previously, isoform 1 RTA has also been shown to act directly through host transcription factors such as RBP-Jk, SP1, and Oct-1, and the failure of alternative isoform to transactivate to a similar level may be a failure to associate with these factors (46, 83–85). We further addressed the failure of RTA isoform 4 to transactivate the k-bZIP promoter by analyzing 293T cells harboring a latent KSHV genome with a mutant Orf50 (preventing the expression of other RTA isoforms which would have confounded these analyses). As seen in the absence of other viral proteins, RTA isoform 4 also failed to induce k-bZIP to high levels, even when the cells were simultaneously exposed to TPA treatment (Fig. 7A). Clearly, this is a very limited analysis, and the complexity of the different RTA isoforms to transactivate viral and cellular promoters in the presence of other viral proteins is an area that warrants further study.

In another limited analysis, we assessed whether RTA transcriptional activation in conjunction with RBP-Jk was unique to RTA isoform 1. To do this, we assessed the activation of the KSHV gene 57 promoter by RTA isoforms 1 and 4 (Fig. 9). This analysis demonstrated that mutation of the defined RRE and/or the RBP-Jk sites had a similar impact on both RTA isoform 1 and RTA isoform 4 activation of the gene 57 promoter, even though RTA isoform 4 activation of this promoter was nearly 10-fold weaker than that observed with RTA isoform 1. Further studies are needed to determine why the different isoforms exhibit distinct transcriptional activation potential, which could reflect an alteration in DNA binding affinity and/or the stability of interactions with other viral and/or cellular proteins.

In summary, our findings extend our understanding of the complex Orf50 region of the KSHV genome. We were able to identify three previously unknown transcripts and two previously unknown promoters and to begin studies to investigate the function of the newly identified RTA isoforms. The generation of RTA isoforms is critical in our understanding of the gammaherpesvirus life cycle. This is especially true in light of the fact that the new RTA isoforms behave in a manner that differs from the previously well-characterized RTA isoform 1. Our working model of KSHV transcription now includes transcriptional interference, the expression of RTA isoforms with variable transactivation potential, multiple promoters that can potentially respond to different cellular signals, and a possible mechanism to aid in the establishment of latency. These newly identified RTA isoforms greatly change the landscape of KSHV life cycle progression.

MATERIALS AND METHODS

Cell culture. 293T (human embryonic kidney) cells, Vero-Cre cells (African green monkey kidney epithelial cells), NIH 3T12 (BALB/c murine fibroblasts), RAW 264.7 (murine macrophages), and 293TΔ50BAC cells (293T cells containing stably transfected bacterial artificial chromosome [BAC] missing the Orf50 region [19]) were maintained in Dulbecco modified Eagle medium (DMEM) supplemented with 10% fetal calf serum, 100 U of penicillin per ml, 100 U of streptomycin per ml, and 2 mM L-glutamine (cMEM). Stably transfected BACs in 293TΔ50BAC cells were maintained through the addition of 1 mg of hygromycin per ml. BCBL-1 (PEL KSHV$^+$ EBV$^-$) cells were maintained in Roswell Park Memorial Institute medium (RPMI) supplemented with 10% fetal calf serum, 100 U of penicillin per ml, 100 U of streptomycin per ml, and 2 mM L-glutamine (cRPMI). To induce lytic reactivation, cells were treated with 25 ng of 12-*O*-tetradecanoylphorbol-13-acetate (TPA; Sigma) per ml. All cells were maintained at 37°C in a tissue culture incubator containing 5% CO_2.

RNA and DNA extraction. DNA extraction was conducted using the basic preparation of genomic DNA from the mammalian tissue protocol. Cells suspensions were centrifuged for 5 min at 500 × *g* at 4°C, and the supernatant was discarded. The cells were then resuspended in 1 volume of digestion buffer (100 mM NaCl, 10 mM Tris-Cl [pH 8], 25 mM EDTA [pH 8], 0.5% sodium dodecyl sulfate [SDS], and 0.1 mg of proteinase K/ml) for 12 to 18 h with shaking at 50°C. After incubation, the samples were extracted using an equal volume of chloroform while centrifuging them for 10 min at 1,700 × *g*. After centrifugation, the aqueous top layer was transferred to a new tube, and a 1/2 volume of 7.5 M ammonium acetate and 2 volumes (of original top layer amount) of 100% ethanol were added. This precipitate was centrifuged at 1,700 × *g* for two additional minutes. Pelleted DNA was rinsed with 70% ethanol and spun at 1,700 × *g* for 2 min, and the supernatant was removed. DNA is resuspended at 1 mg/ml in Tris-EDTA (TE) buffer. The final DNA solution was stored at 4°C. RNA extractions were performed using TRIzol reagent (Invitrogen) or a Pure-Link RNA minikit (Invitrogen). Briefly, the cells were pelleted at 2,000 × *g* for 10 min at 4°C. The supernatant was removed, and either 1 ml of TRIzol was added or the cell pellets were stored at −80°C. If TRIzol was added, 300 μl of chloroform was also added, and the cells were vortexed for 30 s and incubated for 10 min at room temperature. The cells were then centrifuged at 12,000 × *g* for 20 min at 4°C. The top aqueous layer was removed, and 1 ml of isopropanol was added. The cells were shaken and incubated for 10 min at room temperature before being subjected to centrifugation at 12,000 × *g* for 10 min at 4°C. The supernatant was removed, and the cells washed with 1 ml of 75% ethanol, followed by incubation for 10 min at room temperature. Finally, the cells were centrifuged at 12,000 × *g* for 5 min at 4°C, the supernatant was removed, and the RNA was resuspended in an appropriate volume of TE buffer. For the Pure-Link RNA minikit extraction, frozen cell pellets (−80°C) were resuspended in lysis buffer, passaged through a 21-gauge needle 10 times, and subjected to column purification and washing. All RNA was used immediately or stored in 75% ethanol at −80°C.

RACE analysis and primer walking. BCBL-1 cells were plated at 2 × 10^5 cells per ml and treated 24 h later with 25 ng of TPA/ml. Total RNA from BCBL-1 cells was collected at 24, 48, and 72 h after TPA treatment as described above. One microgram of RNA was treated with DNase I (Invitrogen) and subjected to 5′ rapid amplification of cDNA ends (RACE) performed using the GeneRacer system (Invitrogen). RACE-ready cDNA was generated using Superscript III (Invitrogen) reverse transcription with random primers according to the kit's instructions. RACE-ready cDNA was used to look for additional 5′ transcripts through the use of a nested PCR utilizing Platinum *Taq* (Invitrogen). Nested PCR was performed using the 5′ universal forward RACE primer bound to the 5′-RACE tag, either universal primer 1 for round 1 or universal primer 2 for round 2 nested PCR and various reverse primers located in the Orf50 region: E2KSHVR1 (5′-cctccgattgcagacgagtc-3′), E2KSHVR2 (5′-aacatgttaatgtctgtaaacaga-3′), E2KSHVR3 (5′-tgcacacatcttccaccactct-3′), E2KSHVR4 (5′-cgtccgagaggccgacgaagct-3′), E1KSHVR1 (5′-tggctgcctggacagtattc-3′), and E1KSHVR2 (5′-ccttgcggagtaaggttgac-3′). For 5′ primer walking, a universal reverse primer located in exon 2 (E2KSHVR4) was used in conjunction with a series of forward primers every 50 bp, starting at the 5′ end of E1. The following cycling conditions were used for all PCRs: 1 μl of cDNA in a 50-μl PCR mixture at 95°C for 2 min; 30 cycles of denaturing at 94°C for 30 s, annealing at 58°C for 30 s, and extension at 70°C for 2 min; and a final extension at 70°C for 10 min. Round 2 nested amplification was performed with 2 μl of the round 1 PCR product, and the cycling conditions remained the same. PCR products were visualized through the use of a 1% ethidium bromide gel, and excised bands were purified using a Geneclean II kit (MP Biomedicals). Purified PCR products were ligated into a pGEM-T Easy vector system (Promega), transformed into *Escherichia coli*, purified using a DNA miniprep kit (Qiagen), and analyzed by DNA sequencing (Macrogen USA).

Cloning and reporter plasmid generation. DNA from BCBL-1 cells was extracted as previously described. BCLB-1 DNA was used as a template for the amplification of viral promoter constructs in which the promoters were then cloned into a pGL4.10[luc] reporter constructs (Promega). GoTaq (Promega) was used with the following cycling parameters for all promoter amplifications: 95°C for 2 min; 30 cycles of denaturing at 94°C for 30s, annealing at 58°C for 30 s, and extension at 72°C for 30 s; and a final extension at 70°C for 10 min. Standard single-round PCR was used to generate the following constructs using the primers listed. KSHVE1pRBgl2 (5′-actgAGATCTtgtcattgccacccagctac-3′ [restriction digest sites are in uppercase]) reverse primer was used with KSHVE1pF1000Nhe1 (5′-actgGCTAGCcggtttctctaattgcatca-3′), KSHVE1pF500Nhe1 (5′-actgGCTAGCacccacaggcctgttccagt-3′), KSHVE1pF250Nhe1 (5′-actgGCTAGCaatacgctcggtcttgacga-3′), and KSHVE1pF100Nhe1 (5′-actgGCTAGCccataggacccagctacagc-3′) forward primers to generate exon 1 promoter constructs 1,000, 500, 250, and 100 bp in length. KSHVE0aBRBgl2 (5′-actgAGATCTcttgcttgcccggatacgcg-3′) reverse primer was used with KSHVE0aBF1000Nhe1 (5′-actgGCTAGCctgctgcttttagccccgagt-3′), KSHVE0aBF500Nhe1 (5′-actgGCTAGCcctggttcggtgctccccag-3′), KSHVE0aB-F250Nhe1 (5′-actgGCTAGCtgtcacacgtctggctgaga-3′), and KSHVE0aBF100Nhe1 (5′-actgGCTAGCtgtccatacgggccgtgtgc-3′) forward

primers to generate exon 0 promoter constructs 1,000, 500, 250, and 100 bp in length. KSHVN3N4RBgl2 (5′-actgAGATCTaaggggctccctggggagc-3′) reverse primer was used with KSHVN3N4F1000Nhe1 (5′-actgGC TAGCaacacaccctggcgagccca-3′), KSHVN3N4F500Nhe1 (5′-actgGCTAGCtaacagaacctgtccggttc-3′), KSHVN3N4 F250Nhe1 (5′-actgGCTAGCtcgcagcttggctatacaga-3′), and KSHVN3N4-F100Nhe1 (5′-actgGCTAGCggtggtccaca ggacggcaa-3′) forward primers to generate exon N3/N4 promoter constructs 1,000, 500, 250, and 100 bp in length. Finally, KSHVN5RBgl2 (5′-actgAGATCTgccatgaaccggacaggttc-3′) reverse primer was used with KSHVN5F1000Nhe1 (5′-actgGCTAGCgcgaggcgctccttcaattg-3′), KSHVN5F500Nhe1 (5′-actgGCTAGCcgaggcacc cgtgggaagga-3′), KSHVN5F250Nhe1 (5′-actgGCTAGCctgtctgagcagcgagagca-3′), and KSHVN5-F100Nhe1 (5′-actgGCTAGCcatgttgaacttatttttccc-3′) to generate exon N5 promoter constructs of 1,000, 500, 250, and 100 bp in length. In addition, the complete KSHV genome promoter set (32) was kindly provided by Y. Izumiya, and when applicable the primer pairs used to amplify KSHV promoters were the same. For the generation of truncated KSHV promoters ORF59 and ORF4, the following primers were used. Orf59RBgl2 (5′-gctaAGATCT ttgcggccgtagacgcac-3′) reverse primer was used with Orf59-507FKpn1 (5′-gctaGGTACCgtgccttgccaacgatta-3′), Orf59-407FKpn1 (5′-gctaGGTACCcacgcagaggtccaggcg-3′), Orf59-307FKpn1 (5′-gctaGGTACCtccggaggttcc tggaag-3′), Orf59-207FKpn1 (5′-gctaGGTACCcaccggcagtttcaaggc-3′), and Orf59-107FKpn1 (5′-gctaGGTACCa cacttccacctcccta-3′) forward primers. Orf4Bgl2 (5′-gctaAGATCTgctgtaagtagcacggtt-3′) reverse primer was used with Orf4-500FKpn1 (5′-gctaGGTACCccagaaactcatactgta-3′), Orf4-400FKpn1 (5′-gctaGGTACCttgtagtgaa agaagcaa-3′), Orf4-300FKpn1 (5′-gctaGGTACCaggaactattatctttgc-3′), Orf4-200FKpn1 (5′-gctaGGTACCgaagact atacgcaacca-3′), and Orf4-100FKpn1 (5′-gctaGGTACCaaatgttttatgcaaaat-3′) forward primers. For the generation of Orf57 RBP-Jk and RRE mutants, the following primers were used for overlapping PCR to generate mutations. ORF57FNheI (5′-TGCAgctagcAAGACCATTAGCTATC-3′) and ORF57RHindIII (5′-tgcaAAGCTTcttgtac catgtcctttg-3′) were used as forward and reverse outside primers. ORF57RREF (5′-gcaagtgGCCTCGtaatgttcc cacg-3′) and ORF57RRER (5′-gaacattaCGAGGCcacttgctggca-3′) were used for the RRE mutation, ORF57RBPJF (5′-acaataatgtATTAacggcccatttttc-3′) and ORF57RBPJR (5′-aaatgggccgtTAATacattattgttac-3′) were used for the RBP-Jk mutation, and ORF57BothF (5′-agcaagtgGCCTCGtaatgtATAAacggcccatt-3′) and ORF57BothR (5′-tgggccgtTTATacattaCGAGGCcacttgctgg-3′) were used for the RRE/RBP-Jk dual mutation. All of these PCR products were gel purified and cut using either NheI, KpnI, HindIII, or BglII (all from NEB) restriction enzymes depending on the promoter sequence. In addition, the luciferase reporter construct pGL4.10[luc] (Promega) was also digested with these enzymes accordingly. After 1 h of digestion, the plasmid was also treated for 30 min with calf intestinal phosphate (NEB). The digested products and the vector were gel purified again, resuspended in TE buffer, and ligated together for 1 h using T4 DNA ligase (NEB) at room temperature. Ligation products were transformed into Top10 chemically competent cells, and the colonies were screened for the presence of correct promoter orientation within the pGL4.10[luc] vector through DNA sequencing. Clones containing the correct insert and orientations were cultured to high levels, and plasmid DNA was isolated using an Endo-Free maxikit (Qiagen). To assemble the KSHV promoter library, 2.5 μg of promoter DNA was transformed into Top10 chemically competent cells, and colonies were grown on plates and then prepped using the ZR plasmid Endo-Free Mini-Prep kit (Zymo Research) and, before use, the correct promoter and plasmid sequence was determined by sequencing.

The process of generating expression constructs followed a protocol similar to that used for the generation of the reporter constructs. BCBL-1 RNA was extracted as previously described and treated with DNase I (Invitrogen), and 1 μg of RNA was used to generate cDNA using Superscript III (Invitrogen). This cDNA was used as a template for the generation of E1-E2, E2ATG E0a-E2, E0b-E2, and N5-E2 expression constructs. These constructs were generated using the same reverse primer KSHVE2Xho1R (5′-gcatCTCGAGgtctcggaagtaattacgcc-3′), while E1-E2 used the forward primer KSHVE1Not1F (5′-cgtaG CGGCCGCatggcgcaagatgacaaggg-3′), E2ATG used the forward primer KSHVE2AtgNot1F (5′-cgtaGCGGC CGCatgaaagaatgttccaagct-3′), E0a-E2 used the forward primer KSHVE0ANot1F (5′-cgtaGCGGCCGCatgg gcgggtgggtgacaggtaagaagcttcggcggtcctgtgtggaa-3′), E0b-E2 used the forward primer KSHVE0BNot1F (5′-cgtaGCGGCCGCatgcatgactccaaccgtctcacgtccgagggtaagaagcttcggcggtcctgtgtggaa-3′), and finally N5-E2 used the forward primer KSHVN5Not1F (5′-cgtaGCGGCCGCatgcctgaattgcgcaacat-3′). Platinum *Taq* (Invitrogen) using the following cycling parameters was used: 95°C for 2 min; 40 cycles of denaturing at 94°C for 30s, annealing at 64°C for 30 s, and extension at 72°C for 3 min; and a final extension at 72°C for 10 min. PCR products were gel purified, cut using NotI and XhoI, while at the same time also cutting the expression vector pCMV-Tag2B (Stratagene). These restriction-digested products were gel purified and ligated, and constructs were generated as described above.

Luciferase assay and transfections. Transfection of 293T, Vero, 3T12, 293TΔ50BAC, and RAW 264.7 cells was performed in 6- or 12-well plates. One day prior to transfection, the cells were plated at 2×10^5 cells (6-well plates), 1×10^5 cells (12-well plates), or (for RAW 264.7 cells) 1×10^6 cells in cMEM. Transfection mixtures were prepared using either 2.5 μg of reporter plasmid for single transfection or 1.5 μg of reporter plasmid and 1 μg of expression plasmid for dual transfections in 6-well plates and 500 ng of reporter plasmid and 500 ng of expression plasmid for 12-well plates. Transfections were performed using LT-1 transfection reagent (Mirus) according to the manufacturer's instructions. Briefly, 250 μl (6 well) or 100 μl (12 well) of DMEM was used for each transfection well, and the appropriate amount of DNA was added; 7.5 μl of LT-1 per well (6 well) and 3 μl of LT-1 per well (12 well) were added to the media and mixed briefly. The solution was incubated at room temperature for 30 min and then dropwise added to cells. pGL4.13[luc] was used as a positive control. For assay mixtures using an external stimulus, 25 ng of TPA/ml was used. Luciferase assays were performed by lysing cells and using 10 μl of lysate in 50 μl of luciferase agent (1.5 mM HEPES [pH 8], 80 μM $MgSO_4$, 0.4 mM dithiothreitol, 2 μM EDTA, 10.6 μM ATP, 5.4 μM coenzyme A, and 9.4 μM beetle luciferin). Luciferase assays were read using a TD-20/20 luminometer (Turner Biosystems). All transfections were repeated in triplicate, and the results are

presented either as the fold change versus empty pGL4.10[luc] vector or as the fold change versus reporter vector plus empty pCMV-Tag2B vector, unless otherwise indicated.

Immunoblotting. A total of 2×10^5 293TΔ50BAC cells were plated in six-well plates and allowed to grow for 24 h overnight. The cells were then transfected as described above and, at 24, 48, and 72 h posttransfection, the cells were washed with 1× phosphate-buffered saline and lysed in 40 μl of lysis buffer containing 150 mM NaCl, 50 mM Tris-HCl, 1 mM EDTA, and 0.1% Triton X-100 supplemented with 1 mM NaF, 1 mM Na_3VO_4, and EDTA-free protease inhibitor tablet (Roche) for 30 min at 4°C. Protein quantifications were carried out using a DC protein assay (Bio-Rad). For all blots, equal amounts of protein were loaded with 6× SDS loading buffer, boiled for 5 min at 100°C, and run on an SDS-PAGE gel. Proteins were transferred to Hybond-ECL nitrocellulose membranes (Amersham Biosciences) using a Trans-Blot Turbo transfer system (Bio-Rad). After transfer, the blots were blocked in 5% milk in Tris-buffered saline (TBS)-Tween for 1 h at room temperature. After 1 h, the blots were washed three times with TBS-Tween and subjected to primary antibody blotting in 5% milk in TBS overnight at 4°C. The following primary antibodies were used: monoclonal anti-Flag M2-HRP (Sigma) at 1:1,000 and primary mouse monoclonal β-actin antibody (Sigma) at 1:5,000. After three washes with TBS-Tween for 30 min each time, a secondary donkey anti-mouse antibody (Jackson ImmunoResearch), if necessary, was used at 1:2,000 at 4°C for 1 h. The blot was washed again with TBS-Tween three times, and detection was performed by the addition of SuperSignal West Pico chemiluminescent substrate (Pierce). Blots were stripped for reuse using Restore Plus Western blot stripping buffer (Thermo Scientific).

RTA competition assays. Assays were conducted in a manner similar to that used for the luciferase assays described above. Briefly, 293T cells were plated in six-well plates at a concentration of 2×10^5; after 24 h, LT-1 (Mirus) transfection with either Orf60 or Orf28 pGL4.10[luc] KSHV reporter constructs was prepared. A steady 100 ng of reporter construct was transfected under various conditions. First, 400 ng of isoform 1, 2, 3, or 4 expression construct alone, as well as 2 μg of pCMV-Tag2B empty vector plasmid, was transfected with each promoter. Next, 400 ng of isoform 1 was transfected with either 250 ng, 500 ng, or 1 μg of isoform 2, 3, or 4 expression constructs, with total transfected DNA kept to a steady 2.5 μg through the transfection of pCMV-Tag2B empty vector plasmid. After 48 h, competition assays were run and plotted similarly to the luciferase assays described above.

REFERENCES

1. Kedes DH, Operskalski E, Busch M, Kohn R, Flood J, Ganem D. 1996. The seroepidemiology of human herpesvirus 8 (Kaposi's sarcoma-associated herpesvirus): distribution of infection in KS risk groups and evidence for sexual transmission. Nat Med 2:918–924. https://doi.org/10.1038/nm0896-918.
2. Lennette ET, Blackbourn DJ, Levy JA. 1996. Antibodies to human herpesvirus type 8 in the general population and in Kaposi's sarcoma patients. Lancet 348:858–861. https://doi.org/10.1016/S0140-6736(96)03240-0.
3. Rickinson AB. 1996. Changing seroepidemiology of HHV-8. Lancet 348:1110–1111. https://doi.org/10.1016/S0140-6736(05)65265-8.
4. Rohner E, Wyss N, Trelle S, Mbulaiteye SM, Egger M, Novak U, Zwahlen M, Bohlius J. 2014. HHV-8 seroprevalence: a global view. Syst Rev 3:11. https://doi.org/10.1186/2046-4053-3-11.
5. Cesarman E. 2011. Gammaherpesvirus and lymphoproliferative disorders in immunocompromised patients. Cancer Lett 305:163–174. https://doi.org/10.1016/j.canlet.2011.03.003.
6. Cesarman E, Chang Y, Moore PS, Said JW, Knowles DM. 1995. Kaposi's sarcoma-associated herpesvirus-like DNA sequences in AIDS-related body-cavity-based lymphomas. N Engl J Med 332:1186–1191. https://doi.org/10.1056/NEJM199505043321802.
7. Chang Y, Cesarman E, Pessin MS, Lee F, Culpepper J, Knowles DM, Moore PS. 1994. Identification of herpesvirus-like DNA sequences in AIDS-associated Kaposi's sarcoma. Science 266:1865–1869. https://doi.org/10.1126/science.7997879.
8. Ogawa Y, Watanabe D, Hirota K, Ikuma M, Yajima K, Kasai D, Mori K, Ota Y, Nishida Y, Uehira T, Mano M, Yamane T, Shirasaka T. 2014. Rapid multiorgan failure due to large B-cell lymphoma arising in human herpesvirus-8-associated multicentric Castleman's disease in a patient with human immunodeficiency virus infection. Internal Med 53:2805–2809. https://doi.org/10.2169/internalmedicine.53.2212.
9. Cavallin LE, Goldschmidt-Clermont P, Mesri EA. 2014. Molecular and cellular mechanisms of KSHV oncogenesis of Kaposi's sarcoma associated with HIV/AIDS. PLoS Pathog 10:e1004154. https://doi.org/10.1371/journal.ppat.1004154.
10. Noel JC, De Thier F, Heenen M, Fayt I, Abramowicz D, Doutrelepont JM. 1997. HHV-8 is associated with recurrent Kaposi's sarcoma in a renal transplant recipient. Transpl Int 10:81–82. https://doi.org/10.1111/j.1432-2277.1997.tb00543.x.
11. Ertl R, Korb M, Langbein-Detsch I, Klein D. 2015. Prevalence and risk factors of gammaherpesvirus infection in domestic cats in Central Europe. Virol J 12:146. https://doi.org/10.1186/s12985-015-0381-6.
12. Lecis R, Tocchetti M, Rotta A, Naitana S, Ganges L, Pittau M, Alberti A. 2014. First gammaherpesvirus detection in a free-living Mediterranean bottlenose dolphin. J Zoo Wildl Med 45:922–925. https://doi.org/10.1638/2014-0019.1.
13. Bodewes R, Contreras GJ, Garcia AR, Hapsari R, van de Bildt MW, Kuiken T, Osterhaus AD. 2015. Identification of DNA sequences that imply a novel gammaherpesvirus in seals. J Gen Virol 96:1109–1114. https://doi.org/10.1099/vir.0.000029.
14. Wilcox RS, Vaz P, Ficorilli NP, Whiteley PL, Wilks CR, Devlin JM. 2011. Gammaherpesvirus infection in a free-ranging eastern grey kangaroo (Macropus giganteus). Aust Vet J 89:55–57. https://doi.org/10.1111/j.1751-0813.2010.00662.x.
15. Karlin S, Mocarski ES, Schachtel GA. 1994. Molecular evolution of herpesviruses: genomic and protein sequence comparisons. J Virol 68:1886–1902.
16. Virgin HWt, Latreille P, Wamsley P, Hallsworth K, Weck KE, Dal Canto AJ, Speck SH. 1997. Complete sequence and genomic analysis of murine gammaherpesvirus 68. J Virol 71:5894–5904.
17. Pavlova IV, Virgin HW, Speck SH. 2003. Disruption of gammaherpesvirus 68 gene 50 demonstrates that Rta is essential for virus replication. J Virol 77:5731–5739. https://doi.org/10.1128/JVI.77.10.5731-5739.2003.
18. Wu TT, Tong L, Rickabaugh T, Speck S, Sun R. 2001. Function of Rta is essential for lytic replication of murine gammaherpesvirus 68. J Virol 75:9262–9273. https://doi.org/10.1128/JVI.75.19.9262-9273.2001.
19. Xu Y, AuCoin DP, Huete AR, Cei SA, Hanson LJ, Pari GS. 2005. A Kaposi's sarcoma-associated herpesvirus/human herpesvirus 8 ORF50 deletion mutant is defective for reactivation of latent virus and DNA replication. J Virol 79:3479–3487. https://doi.org/10.1128/JVI.79.6.3479-3487.2005.
20. Sun R, Lin SF, Staskus K, Gradoville L, Grogan E, Haase A, Miller G. 1999. Kinetics of Kaposi's sarcoma-associated herpesvirus gene expression. J Virol 73:2232–2242.
21. Gradoville L, Gerlach J, Grogan E, Shedd D, Nikiforow S, Metroka C, Miller G. 2000. Kaposi's sarcoma-associated herpesvirus open reading frame 50/Rta protein activates the entire viral lytic cycle in the HH-B2 primary effusion lymphoma cell line. J Virol 74:6207–6212. https://doi.org/10.1128/JVI.74.13.6207-6212.2000.
22. Lukac DM, Renne R, Kirshner JR, Ganem D. 1998. Reactivation of Kaposi's sarcoma-associated herpesvirus infection from latency by expression of

the ORF 50 transactivator, a homolog of the EBV R protein. Virology 252:304–312. https://doi.org/10.1006/viro.1998.9486.
23. Sun R, Lin SF, Gradoville L, Yuan Y, Zhu F, Miller G. 1998. A viral gene that activates lytic cycle expression of Kaposi's sarcoma-associated herpesvirus. Proc Natl Acad Sci U S A 95:10866–10871. https://doi.org/10.1073/pnas.95.18.10866.
24. Rickabaugh TM, Brown HJ, Wu TT, Song MJ, Hwang S, Deng H, Mitsouras K, Sun R. 2005. Kaposi's sarcoma-associated herpesvirus/human herpesvirus 8 RTA reactivates murine gammaherpesvirus 68 from latency. J Virol 79:3217–3222. https://doi.org/10.1128/JVI.79.5.3217-3222.2005.
25. Chang PJ, Shedd D, Gradoville L, Cho MS, Chen LW, Chang J, Miller G. 2002. Open reading frame 50 protein of Kaposi's sarcoma-associated herpesvirus directly activates the viral PAN and K12 genes by binding to related response elements. J Virol 76:3168–3178. https://doi.org/10.1128/JVI.76.7.3168-3178.2002.
26. Byun H, Gwack Y, Hwang S, Choe J. 2002. Kaposi's sarcoma-associated herpesvirus open reading frame (ORF) 50 transactivates K8 and ORF57 promoters via heterogeneous response elements. Mol Cells 14:185–191.
27. Pavlova I, Yulin C, Speck S. 2005. Murine gammaherpesvirus 68 Rta-dependent activation of the gene 57 promoter. Virology 333:169–179. https://doi.org/10.1016/j.virol.2004.12.021.
28. Wang SE, Wu FY, Yu Y, Hayward GS. 2003. CCAAT/enhancer-binding protein-alpha is induced during the early stages of Kaposi's sarcoma-associated herpesvirus (KSHV) lytic cycle reactivation and together with the KSHV replication and transcription activator (RTA) cooperatively stimulates the viral RTA, MTA, and PAN promoters. J Virol 77:9590–9612. https://doi.org/10.1128/JVI.77.17.9590-9612.2003.
29. Bowser BS, Morris S, Song MJ, Sun R, Damania B. 2006. Characterization of Kaposi's sarcoma-associated herpesvirus (KSHV) K1 promoter activation by Rta. Virology 348:309–327. https://doi.org/10.1016/j.virol.2006.02.007.
30. Haque M, Chen J, Ueda K, Mori Y, Nakano K, Hirata Y, Kanamori S, Uchiyama Y, Inagi R, Okuno T, Yamanishi K. 2000. Identification and analysis of the K5 gene of Kaposi's sarcoma-associated herpesvirus. J Virol 74:2867–2875. https://doi.org/10.1128/JVI.74.6.2867-2875.2000.
31. Deng H, Young A, Sun R. 2000. Auto-activation of the rta gene of human herpesvirus-8/Kaposi's sarcoma-associated herpesvirus. The J Gen Virol 81:3043–3048. https://doi.org/10.1099/0022-1317-81-12-3043.
32. Ellison TJ, Izumiya Y, Izumiya C, Luciw PA, Kung HJ. 2009. A comprehensive analysis of recruitment and transactivation potential of K-Rta and K-bZIP during reactivation of Kaposi's sarcoma-associated herpesvirus. Virology 387:76–88. https://doi.org/10.1016/j.virol.2009.02.016.
33. Roan F, Inoue N, Offermann MK. 2002. Activation of cellular and heterologous promoters by the human herpesvirus 8 replication and transcription activator. Virology 301:293–304. https://doi.org/10.1006/viro.2002.1582.
34. Deng H, Chu JT, Rettig MB, Martinez-Maza O, Sun R. 2002. Rta of the human herpesvirus 8/Kaposi sarcoma-associated herpesvirus upregulates human interleukin-6 gene expression. Blood 100:1919–1921. https://doi.org/10.1182/blood-2002-01-0015.
35. Gray KS, Allen RD, III, Farrell ML, Forrest JC, Speck SH. 2008. Alternatively initiated gene 50/RTA transcripts expressed during murine and human gammaherpesvirus reactivation from latency. J Virol 83:314–328. https://doi.org/10.1128/JVI.01444-08.
36. Wakeman BS, Johnson LS, Paden CR, Gray KS, Virgin HW, Speck SH. 2014. Identification of alternative transcripts encoding the essential murine gammaherpesvirus lytic transactivator RTA. J Virol 88:5474–5490. https://doi.org/10.1128/JVI.03110-13.
37. Liu S, Pavlova IV, Virgin HWt Speck SH. 2000. Characterization of gammaherpesvirus 68 gene 50 transcription. J Virol 74:2029–2037. https://doi.org/10.1128/JVI.74.4.2029-2037.2000.
38. Wu TT, Usherwood EJ, Stewart JP, Nash AA, Sun R. 2000. Rta of murine gammaherpesvirus 68 reactivates the complete lytic cycle from latency. J Virol 74:3659–3667. https://doi.org/10.1128/JVI.74.8.3659-3667.2000.
39. Reese TA, Wakeman BS, Choi HS, Hufford MM, Huang SC, Zhang X, Buck MD, Jezewski A, Kambal A, Liu CY, Goel G, Murray PJ, Xavier RJ, Kaplan MH, Renne R, Speck SH, Artyomov MN, Pearce EJ, Virgin HW. 2014. Helminth infection reactivates latent gammaherpesvirus via cytokine competition at a viral promoter. Science 345:573–577. https://doi.org/10.1126/science.1254517.
40. Dourmishev LA, Dourmishev AL, Palmeri D, Schwartz RA, Lukac DM. 2003. Molecular genetics of Kaposi's sarcoma-associated herpesvirus (human herpesvirus-8) epidemiology and pathogenesis. Microbiol Mol Biol Rev 67:175–212. https://doi.org/10.1128/MMBR.67.2.175-212.2003.
41. Bu W, Carroll KD, Palmeri D, Lukac DM. 2007. Kaposi's sarcoma-associated herpesvirus/human herpesvirus 8 ORF50/Rta lytic switch protein functions as a tetramer. J Virol 81:5788–5806. https://doi.org/10.1128/JVI.00140-07.
42. Guito J, Lukac DM. 2015. KSHV reactivation and novel implications of protein isomerization on lytic switch control. Viruses 7:72–109. https://doi.org/10.3390/v7010072.
43. Campbell M, Izumiya Y. 2012. Posttranslational modifications of Kaposi's sarcoma-associated herpesvirus regulatory proteins: SUMO and KSHV. Front Microbiol 3:31.
44. Shearwin KE, Callen BP, Egan JB. 2005. Transcriptional interference: a crash course. Trends Genet 21:339–345. https://doi.org/10.1016/j.tig.2005.04.009.
45. Puglielli MT, Desai N, Speck SH. 1997. Regulation of EBNA gene transcription in lymphoblastoid cell lines: characterization of sequences downstream of BCR2 (Cp). J Virol 71:120–128.
46. Carroll KD, Khadim F, Spadavecchia S, Palmeri D, Lukac DM. 2007. Direct interactions of Kaposi's sarcoma-associated herpesvirus/human herpesvirus 8 ORF50/Rta protein with the cellular protein octamer-1 and DNA are critical for specifying transactivation of a delayed-early promoter and stimulating viral reactivation. J Virol 81:8451–8467. https://doi.org/10.1128/JVI.00265-07.
47. Izumiya Y, Lin SF, Ellison T, Chen LY, Izumiya C, Luciw P, Kung HJ. 2003. Kaposi's sarcoma-associated herpesvirus K-bZIP is a coregulator of K-Rta: physical association and promoter-dependent transcriptional repression. J Virol 77:1441–1451. https://doi.org/10.1128/JVI.77.2.1441-1451.2003.
48. Liu Y, Cao Y, Liang D, Gao Y, Xia T, Robertson ES, Lan K. 2008. Kaposi's sarcoma-associated herpesvirus RTA activates the processivity factor ORF59 through interaction with RBP-Jκ and a *cis*-acting RTA responsive element. Virology 380:264–275. https://doi.org/10.1016/j.virol.2008.08.011.
49. Persson LM, Wilson AC. 2010. Wide-scale use of Notch signaling factor CSL/RBP-Jκ in RTA-mediated activation of Kaposi's sarcoma-associated herpesvirus lytic genes. J Virol 84:1334–1347. https://doi.org/10.1128/JVI.01301-09.
50. Wen HJ, Minhas V, Wood C. 2009. Identification and characterization of a new Kaposi's sarcoma-associated herpesvirus replication and transcription activator (RTA)-responsive element involved in RTA-mediated transactivation. J Gen Virol 90:944–953. https://doi.org/10.1099/vir.2008.006817-0.
51. Liang Y, Chang J, Lynch SJ, Lukac DM, Ganem D. 2002. The lytic switch protein of KSHV activates gene expression via functional interaction with RBP-Jκ (CSL), the target of the Notch signaling pathway. Genes Dev 16:1977–1989. https://doi.org/10.1101/gad.996502.
52. Koenigsberger C, Chicca JJ, II, Amoureux MC, Edelman GM, Jones FS. 2000. Differential regulation by multiple promoters of the gene encoding the neuron-restrictive silencer factor. Proc Natl Acad Sci U S A 97:2291–2296. https://doi.org/10.1073/pnas.050578797.
53. Breslin MB, Geng CD, Vedeckis WV. 2001. Multiple promoters exist in the human GR gene, one of which is activated by glucocorticoids. Mol Endocrinol 15:1381–1395. https://doi.org/10.1210/mend.15.8.0696.
54. Kuhn K, Weihe A, Borner T. 2005. Multiple promoters are a common feature of mitochondrial genes in Arabidopsis. Nucleic Acids Res 33:337–346. https://doi.org/10.1093/nar/gki179.
55. Xin D, Hu L, Kong X. 2008. Alternative promoters influence alternative splicing at the genomic level. PLoS One 3:e2377. https://doi.org/10.1371/journal.pone.0002377.
56. Bodescot M, Perricaudet M, Farrell PJ. 1987. A promoter for the highly spliced EBNA family of RNAs of Epstein-Barr virus. J Virol 61:3424–3430.
57. Rogers RP, Woisetschlaeger M, Speck SH. 1990. Alternative splicing dictates translational start in Epstein-Barr virus transcripts. EMBO J 9:2273–2277.
58. Speck SH, Pfitzner A, Strominger JL. 1986. An Epstein-Barr virus transcript from a latently infected, growth-transformed B-cell line encodes a highly repetitive polypeptide. Proc Natl Acad Sci U S A 83:9298–9302. https://doi.org/10.1073/pnas.83.24.9298.
59. Speck SH, Strominger JL. 1985. Analysis of the transcript encoding the latent Epstein-Barr virus nuclear antigen I: a potentially polycistronic message generated by long-range splicing of several exons. Proc Natl Acad Sci U S A 82:8305–8309. https://doi.org/10.1073/pnas.82.24.8305.
60. Woisetschlaeger M, Yandava CN, Furmanski LA, Strominger JL, Speck SH. 1990. Promoter switching in Epstein-Barr virus during the initial stages

of infection of B lymphocytes. Proc Natl Acad Sci U S A 87:1725–1729. https://doi.org/10.1073/pnas.87.5.1725.
61. Woisetschlaeger M, Strominger JL, Speck SH. 1989. Mutually exclusive use of viral promoters in Epstein-Barr virus latently infected lymphocytes. Proc Natl Acad Sci U S A 86:6498–6502. https://doi.org/10.1073/pnas.86.17.6498.
62. Paulson EJ, Fingeroth JD, Yates JL, Speck SH. 2002. Methylation of the EBV genome and establishment of restricted latency in low-passage EBV-infected 293 epithelial cells. Virology 299:109–121. https://doi.org/10.1006/viro.2002.1457.
63. Schaefer BC, Strominger JL, Speck SH. 1997. Host-cell-determined methylation of specific Epstein-Barr virus promoters regulates the choice between distinct viral latency programs. Mol Cell Biol 17:364–377. https://doi.org/10.1128/MCB.17.1.364.
64. Chubb IW, Goodman S, Smith AD. 1976. Is acetylcholinesterase secreted from central neurons into the cerebral fluid? Neuroscience 1:57–62. https://doi.org/10.1016/0306-4522(76)90048-8.
65. Nicholas J. 2003. Human herpesvirus-8-encoded signaling ligands and receptors. J Biomed Sci 10:475–489. https://doi.org/10.1007/BF02256109.
66. Nicholas J. 2005. Human gammaherpesvirus cytokines and chemokine receptors. J Interferon Cytokine Res 25:373–383. https://doi.org/10.1089/jir.2005.25.373.
67. Rangaswamy US, Speck SH. 2014. Murine gammaherpesvirus M2 protein induction of IRF4 via the NFAT pathway leads to IL-10 expression in B cells. PLoS Pathog 10:e1003858. https://doi.org/10.1371/journal.ppat.1003858.
68. Steed A, Buch T, Waisman A, Virgin HW. 2007. Gamma interferon blocks gammaherpesvirus reactivation from latency in a cell type-specific manner. J Virol 81:6134–6140. https://doi.org/10.1128/JVI.00108-07.
69. Matar CG, Rangaswamy US, Wakeman BS, Iwakoshi N, Speck SH. 2014. Murine gammaherpesvirus 68 reactivation from B cells requires IRF4 but not XBP-1. J Virol 88:11600–11610. https://doi.org/10.1128/JVI.01876-14.
70. Sun CC, Thorley-Lawson DA. 2007. Plasma cell-specific transcription factor XBP-1s binds to and transactivates the Epstein-Barr virus BZLF1 promoter. J Virol 81:13566–13577. https://doi.org/10.1128/JVI.01055-07.
71. Wilson SJ, Tsao EH, Webb BL, Ye H, Dalton-Griffin L, Tsantoulas C, Gale CV, Du MQ, Whitehouse A, Kellam P. 2007. X Box binding protein XBP-1s transactivates the Kaposi's sarcoma-associated herpesvirus (KSHV) ORF50 promoter, linking plasma cell differentiation to KSHV reactivation from latency. J Virol 81:13578–13586. https://doi.org/10.1128/JVI.01663-07.
72. Yu F, Feng J, Harada JN, Chanda SK, Kenney SC, Sun R. 2007. B cell terminal differentiation factor XBP-1 induces reactivation of Kaposi's sarcoma-associated herpesvirus. FEBS Lett 581:3485–3488. https://doi.org/10.1016/j.febslet.2007.06.056.
73. Malik P, Blackbourn DJ, Cheng MF, Hayward GS, Clements JB. 2004. Functional cooperation between the Kaposi's sarcoma-associated herpesvirus ORF57 and ORF50 regulatory proteins. J Gen Virol 85:2155–2166. https://doi.org/10.1099/vir.0.79784-0.
74. Li H, Komatsu T, Dezube BJ, Kaye KM. 2002. The Kaposi's sarcoma-associated herpesvirus K12 transcript from a primary effusion lymphoma contains complex repeat elements, is spliced, and initiates from a novel promoter. J Virol 76:11880–11888. https://doi.org/10.1128/JVI.76.23.11880-11888.2002.
75. Sadler R, Wu L, Forghani B, Renne R, Zhong W, Herndier B, Ganem D. 1999. A complex translational program generates multiple novel proteins from the latently expressed kaposin (K12) locus of Kaposi's sarcoma-associated herpesvirus. J Virol 73:5722–5730.
76. Uppal T, Banerjee S, Sun Z, Verma SC, Robertson ES. 2014. KSHV LANA: the master regulator of KSHV latency. Viruses 6:4961–4998. https://doi.org/10.3390/v6124961.
77. Sun R, Liang D, Gao Y, Lan K. 2014. Kaposi's sarcoma-associated herpesvirus-encoded LANA interacts with host KAP1 to facilitate establishment of viral latency. J Virol 88:7331–7344. https://doi.org/10.1128/JVI.00596-14.
78. Vazquez Ede L, Carey VJ, Kaye KM. 2013. Identification of Kaposi's sarcoma-associated herpesvirus LANA regions important for episome segregation, replication, and persistence. J Virol 87:12270–12283. https://doi.org/10.1128/JVI.01243-13.
79. Verma SC, Lan K, Robertson E. 2007. Structure and function of latency-associated nuclear antigen. Curr Top Microbiol Immunol 312:101–136.
80. Paden CR, Forrest JC, Moorman NJ, Speck SH. 2010. Murine gammaherpesvirus 68 LANA is essential for virus reactivation from splenocytes but not long-term carriage of viral genome. J Virol 84:7214–7224. https://doi.org/10.1128/JVI.00133-10.
81. Xue Z, Ye Q, Anson SR, Yang J, Xiao G, Kowbel D, Glass NL, Crosthwaite SK, Liu Y. 2014. Transcriptional interference by antisense RNA is required for circadian clock function. Nature 514:650–653. https://doi.org/10.1038/nature13671.
82. Camblong J, Beyrouthy N, Guffanti E, Schlaepfer G, Steinmetz LM, Stutz F. 2009. *trans*-Acting antisense RNAs mediate transcriptional gene cosuppression in Saccharomyces cerevisiae. Genes Dev 23:1534–1545. https://doi.org/10.1101/gad.522509.
83. Wang S, Liu S, Wu MH, Geng Y, Wood C. 2001. Identification of a cellular protein that interacts and synergizes with the RTA (ORF50) protein of Kaposi's sarcoma-associated herpesvirus in transcriptional activation. J Virol 75:11961–11973. https://doi.org/10.1128/JVI.75.24.11961-11973.2001.
84. Chen J, Ye F, Xie J, Kuhne K, Gao SJ. 2009. Genome-wide identification of binding sites for Kaposi's sarcoma-associated herpesvirus lytic switch protein, RTA. Virology 386:290–302. https://doi.org/10.1016/j.virol.2009.01.031.
85. West JT, Wood C. 2003. The role of Kaposi's sarcoma-associated herpesvirus/human herpesvirus-8 regulator of transcription activation (RTA) in control of gene expression. Oncogene 22:5150–5163. https://doi.org/10.1038/sj.onc.1206555.